AWARD NUMBER: W81XWH-18-1-0533

TITLE: Targeting Pim Kinase/lncH19 Axis in Enzalutamide Resistant Prostate Cancer

PRINCIPAL INVESTIGATOR: Neha Singh, PhD

CONTRACTING ORGANIZATION: UNIVERSITY OF ARIZONA
TUCSON AZ 85719-4824

REPORT DATE: OCTOBER 2019

TYPE OF REPORT: Annual technical report

PREPARED FOR: U.S. Army Medical Research and Development Command
Fort Detrick, Maryland 21702-5012

REPORT DOCUMENTATION PAGE

Form Approved
OMB No. 0704-0188

1. REPORT DATE	**2. REPORT TYPE**	**3. DATES COVERED**
OCTOBER 2019	Annual	30SEP2018 - 29SEP2019

4. TITLE AND SUBTITLE

Targeting Pim Kinase/lncH19 Axis in Enzalutamide Resistant Prostate Cancer

5a. CONTRACT NUMBER
W81XWH-18-1-0533

5b. GRANT NUMBER
W81XWH1810533

5c. PROGRAM ELEMENT NUMBER

6. AUTHOR(S)
Neha Singh

E-Mail: nehasingh@email.arizona.edu

5d. PROJECT NUMBER

5e. TASK NUMBER

5f. WORK UNIT NUMBER

7. PERFORMING ORGANIZATION NAME(S) AND ADDRESS(ES)

University of Arizona,
Tucson, AZ 85724

8. PERFORMING ORGANIZATION REPORT NUMBER

9. SPONSORING / MONITORING AGENCY NAME(S) AND ADDRESS(ES)

U.S. Army Medical Research and Development Command
Fort Detrick, Maryland 21702-5012

10. SPONSOR/MONITOR'S ACRONYM(S)

11. SPONSOR/MONITOR'S REPORT NUMBER(S)

12. DISTRIBUTION / AVAILABILITY STATEMENT

Approved for Public Release; Distribution Unlimited

Approved for public release

13. SUPPLEMENTARY NOTES

14. ABSTRACT Prostate cancer (PCa) is the most common non-skin cancer in American men and contributes to a leading number of cancer-related mortalities. With the advent of anti-androgen drugs for instance enzalutamide (Enza), most tumors that advance to metastatic castration-resistant PCa develop resistance to this therapy which is generally incurable. There is an urgent need to come up with therapeutic interventions to overcome such resistance. The mechanism of Enza resistance leading to aggressive PCa disease is not very well understood. Recently, the resistance to Enza due to deletions/mutations in the TP53 (p53) and retinoblastoma (Rb) genes have been linked to the overexpression of SOX2 gene - a reprogramming transcription factor; SOX2 knockdown in these cells restores the sensitivity to Enza. In this proposal, we identified a novel signaling cascade showing that Pim kinase, a serine threonine protein kinase that is overexpressed in PCa, control a long noncoding RNA H19 (H19), which in turn regulates the expression of SOX2 along with other stem cell genes, Oct4, Klf4, and Nanog. The knowledge gained through the studies proposed in this application during the first year have unravel mechanistic details of Pim/H19 mediated $p53^{-}/Rb^{-}$ induction of stem cell genes that is responsible for the ADT. Additionally, the rational and novel therapeutic strategies proposed to overcome resistance to Enza by inhibiting the Pim/H19 axis were demonstrated to be effective in PCa cells. As a young investigator award, the career development plan and research support outlined in this proposal is also strengthening my long-term goal of becoming an independent investigator with focus on PCa research.

15. SUBJECT TERMS
Prostate cancer, SOX2, PIM1, long noncoding RNA H19, Stem cells, P53/Rb loss, Resistance mechanisms, Androgen deprivation therapy.

16. SECURITY CLASSIFICATION OF:			**17. LIMITATION OF ABSTRACT**	**18. NUMBER OF PAGES**	**19a. NAME OF RESPONSIBLE PERSON**
a. REPORT	**b. ABSTRACT**	**c. THIS PAGE**			USAMRMC
Unclassified	Unclassified	Unclassified	Unclassified	75	**19b. TELEPHONE NUMBER** *(include area code)*

TABLE OF CONTENTS

1. Introduction

Prostate cancer (PCa) continues to cause leading number of cancer related mortalities in American men. Enzalutamide (Enza), is a chemotherapy drug for the treating PCa, that functions as androgen receptor (AR) inhibitor (1). Although, clinical trials with Enza on CRPC patients have demonstrated antitumor activity, more cases of tumors eventually develop resistance (2). There is an urgent need to come up with therapeutic interventions to overcome resistance that develops to androgen deprivation therapy (ADT). Recently, Enza resistance was shown to occur after cells accumulate deletions/mutations in TP53 (p53) and retinoblastoma (Rb) gene leading to overexpression of Sox2, a gene reprogramming transcription factor, and consequently making them Enza resistant (3,4). Sox2 silencing restores sensitivity to this agent (4). Since direct targeting of Sox2 is not currently clinically feasible, novel drugable targets need to be identified to restore sensitivity to Enza in P53/Rb deleted PCa. Our preliminary results identified a novel signaling cascade that mediates Sox2 overexpression. The goal of this research proposal is to overcome Enza resistance by understanding and targeting the Pim1/H19 pathway. This goal is based on the hypothesis that Pim kinase overexpression in prostate cancer induces H19, which in turn increases Sox2/Oct4/Klf4/Nanog, making these tumor cells basal-like and ADT resistant. Based on this hypothesis, we propose that targeting this pathway would restore the sensitivity to ADT, providing a novel therapeutic approach. The focus of the research carried out in the first year of this grant has been to provide novel insights into the PIM dependent signaling of H19 induced stem cell gene expression in murine prostate organoids with loss of P53/Rb, due to the importance of this pathway in development of resistance to ADT. Secondly, given theses mechanistic insights the therapeutic targeting of PIM/H19 to overcome Enza resistance were also tested under in vitro conditions. This focus was built on the basis of preliminary data collected at the time of the application. The results obtained will pave the way for the second year of the investigation to solidify these mechanisms of PIM/H19/stem cell gene pathway that is important in ADT and testing the therapeutic combination of inhibiting the PIM/H19 axis under ADT. Together, the results delineate a unique signaling cascade driven by the PIM kinases that involves a lncRNA and stem cell genes to regulate tumor growth.

2. Keywords

Prostate cancer, SOX2, PIM1, long noncoding RNA H19, Stem cells, P53/Rb loss, Resistance mechanisms, Androgen deprivation therapy.

3. Accomplishments

The accomplishments in the first year of this grant has been divided for research specific tasks and training accomplishments during this period.

Research specific tasks:

The tasks are outlined and the results have been discussed. Additionally, the importance of major findings under each task has been discussed after each observation. A strategic decision was made to shift some of the Tasks in Specific Aim 1, Major task 5 of year 1 to the year 2 due to low availability of organoid culture in order to perform these. The order of analysis has been tried to keep consistent with the statement of work to enhance the efficacy and validity of the results within the scope and direction of the project. The experiments have been performed in a logical sequence and have led to identifying *a novel pathway controlled by the PIM kinases whose inhibition could impact clinical outcomes. PIM kinase induction increases the lncRNA H19 and this in turn regulates stem cell genes, including the transcription factor SOX2 which plays a role in controlling the response to anti-androgen therapy. Additionally, we demonstrate that the combination of a PIM inhibitor and H19 knockdown can sensitize prostate cancer cells to Enza while also reducing the tumor forming capacity of the highly aggressive NEPC.*

<u>Specific Aim 1: Major task 1: Culture genetically manipulated prostate organoids from GEM mouse models</u>

The task was designed to generate models to test the hypothesis that PIM1/H19 mediates the $P53^{-/-}/Rb^{-/-}$ induction of stem cell genes. I was able to successfully isolate the prostate from Wild type, $P53^{flox/flox}/Rb^{flox/flox}$, $P53^{flox/flox}/Rb^{flox/flox}$ x probasin cre mice (**Figure 1a**). The prostate tissues where then individually dissociated using collagenase and trypsin via previously established protocols (5) and then cultured in the EGF/Noggin/R-Spondin media in growth factor reduced Matrigel for growth of organoids (Subtask 1) (**Figure 1b**). All studies involving the use of animals were approved by and conducted in accordance with the guidelines of the Institutional Animal Care and Use Committees at the University of Arizona Cancer Center. The murine organoids were replenished with fresh media every 3−4 days during organoid growth. Dense cultures with organoids ranging in size from 200 to 500μm were passaged weekly. Organoid cultures were cryopreserved using Bambanker (Gibco) at −80°C.

Lentiviral particle production and infection was performed as described previously (Tiscornia et al., 2006). The plasmids used for knockdown of human H19 in LNCaP was performed using the lentiviral plasmids pLenti-siH19-GFP (Abm, #i009382) and pLenti-scrambled siRNA-GFP (Abm,

#LV015-G) as a control. These siH19 plasmids allow for direct non-viral plasmid transfection for immediate expression (siH19) and also package into lentiviral particles for high efficiency transduction and stably integrated expression (shH19). Overexpression of human H19 in LNCaP cells was performed using pLenti-GIII-CMV-H19-GFP-2A-Puro (Abm, # LV178008). For H19 knockdown in mouse organoids, plasmid GIPZ Mouse H19 shRNA purchased from Dharmacon (RMM4431), and for Cre recombinase expression, the plasmid FUGW-Cre (Addgene) was used. After the lentivirus of the indicated gene manipulation was produced, we proceeded with the infection/transduction of either adherent PCa cells-LNCaP and/or murine prostate organoids. infection of adherent PCa cells- LNCaP, 10^6 cells/well were seeded in six-well plates and infected with concentrated lentiviral particles 1 day after seeding. For lentiviral transduction, organoids were pre-incubated for at least 48h with regular organoid media supplemented with Wnt-3a and Rho kinase inhibitor (6). After 48h, organoids were dissociated with TrypLE and spinoculated with lentiviral particles along with polybrene (8μM final concentration) at 600g for 1h at 32°C. After incubating organoid cells at 37°C for 3h, the cells were replated in Matrigel in ENR media without lentivirus and allowed to grow for several days. Infected organoids were monitored by fluorescence microscope and successful transductions were indicated by the green fluorescence (for CRE and shH19 conditions) and red fluorescence (for Control and PIM1 conditions) as shown in **Figure 2a** and **Figure 2b** respectively.

In order to confirm the genetic manipulations caused due to the lentiviral transductions, quantitative PCR was performed. Briefly, total RNA was isolated from organoids using TRIzol reagent (Invitrogen, 15596–018). 1μg total RNA were reverse transcribed by using i-Script cDNA Synthesis System kit (Biorad, 1708891). To measure gene expression, Real time PCR was performed using SsoAdvanced™ Universal SYBR® Green Supermix (Biorad, 1725271), following the manufacturer's protocol. Expression level of each transcript was quantified by using Bio-Rad CFX96 Real-Time PCR Detection System. Quantitative real-time PCR (qPCR) assay were performed using the primers for H19, PIM1, KLF4, SOX2, OCT4, NANOG. 18S and HPRT were used as endogenous controls. Details of the primers used and conditions can be found in Appendix B- Materials and methods. The qPCR results demonstrated the desired genetic manipulations as follows:

- Infection with Cre lentivirus induced the double knockdown of P53/Rb expression (**Figure 2c**).
- Infection with shH19 lentivirus caused knockdown of H19 expression (**Figure 2d**).
- Infection of PIM1 lentivirus induced PIM1 overexpression (**Figure 2e**).

Thus through Task 1 in Year 1, we have successfully established organoid cultures from mouse prostate which serve as better cell culture models that closely recapitulate prostate histology. We also induced the desired genetic manipulations and confirmed those changes and these organoid models will help us dissect the role of PIM1/H19 axis in Enzalutamide resistance via the loss of P53/Rb.

Specific Aim 1: Major task 2: Mycoplasma testing of mouse organoid cultures

Mycoplasma testing- Regular testing of mycoplasma contamination was performed in the cell lines and organoids using MycoAlert™ Mycoplasma Detection Kit (LT07-118, Lonza) and only mycoplasma free cells were used for experimentation.

Specific Aim 1: Major task 3: Cell line authentication of mouse organoid cultures and human cell lines

In order to maintain the authenticity and purity of cell lines used for a long time in culture conditions, STR cell line authentication is performed. We are yet to perform cell line authentication on the cell lines that we are using primarily because we are not using a cell line either human or murine for more than 3 months continuously. We take out cryopreserved early passage cell lines for use after that time period. Keeping the cell lines for shorter span of times does not affect the purity and authenticity of the cell lines. However, we plan to check the authenticity of the cells prior to in vivo experiment since those treatments could take longer than the in vitro experiments performed during Year 1.

Specific Aim 1: Major task 4: Test whether Pim/H19 mediates the effect of p53/RB loss on increasing Sox2 in prostate stem cells

This task was designed to test whether PIM/H19 mediate the effect of P53/Rb loss on increasing SOX2 in prostate stem cells.

To test this, organoids generated in Specific aim 1, Task 1 were utilized. To evaluate whether changes in the levels of P53 and Rb1 modulate H19 expression, organoids derived from $Trp53^{flox/flox}/Rb1^{flox/flox}$ mouse prostates were transduced with lentivirus expressing Cre recombinase (Cre-GFP) to generate double-knockout organoids. Organoids transduced with control lentivirus (EV-GFP) were used as control. As demonstrated by qPCR results these DKO organoids demonstrate markedly enhanced expression of H19, as well as the induction of stem cell transcripts (Klf4, Oct4 and Sox2) (**Figure 3c**). To test whether the expression of stem cell genes is through H19 in P53/Rb knockdown cells, we decided to knockdown H19 using shRNA in the CRE organoids. qPCR results demonstrated that the knockdown of H19 in CRE organoids

abrogated the upregulation of stem cell genes (SOX2/OCT4/KLF4/Nanog) (**Figure 3c**) indicating that the lineage plasticity marker SOX2 is indeed controlled by H19 in these P53/Rb double knockout organoids. These findings were confirmed at the protein expression level (**Figure 3d**) with the help of western blots of the proteins extracted from the same organoids used for RNA extraction.

We next tested the relevance of these findings at the phenotypic level by testing the effects of the H19 knockdown on proliferation and invasion of CRE organoids. Aggressive prostate tumors progressing by escaping androgen deprivation therapy (ADT) are characterized by highly proliferative cells with increased metastatic potential (7). To assess the effect of H19 knockdown on the growth of these aggressive prostate tumors, murine organoid (CRE) with or without stable knockdown of H19 was evaluated for organoid growth. While CRE organoids exhibited enhanced proliferation, H19 knockdown significantly inhibited the growth of these ($p=7 \times 10-9$) (**Figure 3a**), demonstrating the essential role of H19 in controlling proliferation in aggressive tumors with P53/Rb loss that could potentially lead to ADT resistance. To examine the ability of H19 to modulate tumor cell invasion, dissociated mouse Trp53/Rb1 DKO organoid cells were placed in a transwell with Flourblock inserts and fluorescence on the bottom of transwell was measured after 5 days (**Figure 3b**). In this model, while the loss of P53/Rb enhanced migration/invasion of murine organoids, knockdown of H19 was able to inhibit their invasive capabilities.

Together this data suggests that a decrease in H19 affects the growth and invasive potential that might be responsible for ADT resistance upon the loss of P53/Rb which are shown to be mediated at least in part by H19 regulation of SOX2 and other stem cell genes.

To evaluate the effect of PIM1 overexpression on growth of normal stem cells, we isolated wild type mouse prostate organoids that have been shown to possess stem cell like characteristics (5). We utilized the PIM1 overexpressing murine organoids as developed in Task1. First, we wanted to observe the phenotypic effects of PIM1 overexpression on organoid proliferation. PIM1 overexpressing and EV control murine prostate organoids were dissociated with TrypLE (Invitrogen) into tiny cell clusters, plated (5000 cell clusters/well) for 4-6 days. A real-time imaging system (IncuCyte™, Essen Bio) was used to measure organoid growth. Images were captured every 12h and results were plotted as the percent average organoid growth versus time. PIM1 overexpression in these organoids caused a significant increase in proliferation of these cells (**Figure 4a** ; PIM1-RFP vs EV-RFP, $p<0.001$). Next, we evaluated the gene expression of stem cell genes and H19 with PIM1 overexpression in these mouse organoids. qPCR results demonstrated that PIM1 overexpression induced increases in H19 as well as the stem cell genes Klf4, Oct-4, and Sox2 (**Figure 4b**).

Thus, experiments conducted in Specific Aim 1 Task 4 year 1, help to establish a novel signaling cascade connecting PIM1, H19, and stem cell genes, suggesting that the PIM1 induction of stem cell genes may occur with the activity of H19. We also prove that the phenotypic effects of increased proliferation and invasion is mediated at least in part by the regulation of SOX2 by H19 in the P53/Rb double knockout organoids and PIM1 in normal organoids.

Specific Aim 1: Major task 5: Mechanism by which p53/Rb and Pim-1 protein kinases regulate H19 levels

We have made a strategic decision to shift the subtask 1 (Bisulphite sequencing) and subtask 2 (Reduced representation Bisulphite sequencing) in Specific Aim 1, Major task 5 of year 1 to the year 2. This was due to requirement of large number of organoid samples needed to investigate the mechanisms by which P53/Rb loss and PIM-1 protein kinase regulate H19 levels. These experiments are key to decipher underlying mechanisms of PIM mediated regulation of H19 and we plan to definitely carry out those experiments once we have generated enough organoids to be confident.

Specific Aim 2: Major task 1: Evaluate whether Pim inhibitors can overcome Enza resistance in stem cell derived tumors in vitro

In the tasks outlined under specific aim 2, we majorly wanted to investigate whether inhibition of PIM/H19 axis was sufficient to overcome Enza resistance.

To further this investigation, it was imperative that we establish that H19 is modulated by Androgen receptor (AR) signaling. We performed a simple experiment where in normal murine organoids, which grow under dihydrotestosterone (DHT- an AR agonist that upregulated androgen signaling), a removal of DHT was performed and qPCR was done on the murine organoids cultured with or without DHT. qPCR results demonstrated that removal of DHT from the organoid media induced a 7 to 10-fold upregulation of H19 expression (**Figure 5a**). *This data suggest that androgen signaling plays a role in regulating H19 expression, and that the blockade of AR induces H19, potentially enhancing the stem cells genes inducing lineage plasticity.*

Patients diagnosed with advanced PCa initially respond to ADT but ultimately develop hormone-refractory disease that leads to death. Recent evidence suggests that increased expression of the reprogramming stem cell transcription factor SOX2 makes PCa cells resistant to hormone blockade by the anti-androgen Enza (4). In order to evaluate if PIM inhibitors could overcome Enza resistance in vitro, we used the organoids as developed in Specific aim1, Task1. Control (EV), P53/Rb knockout (Cre) organoids with or without H19 knockdown (shH19) were dissociated with TrypLE (Invitrogen) into tiny cell clusters, plated (5000 cell clusters/well) and treated under

desired conditions for 4-6 days. The drug treatment conditions were as follows, Enza (5μM, 10μM) and PIM inhibitor (PIM447, 3μM). DMSO was used for control drug treatment. A real-time imaging system (Incucyte) which is more accurate than the MTS assays, was used to measure organoid growth. Images were captured every 12h. The images shown in **Figure 5b** are a compilation of Pim inhibitor and Enza treatment either individually or in combination (as seen on day 5) when added to Control EV and CRE organoids with or without H19 knockdown (shH19). As observed from the images of multiple replicates of the each treatment condition- Enza treatment did not appear to modulate organoid growth in this system. Although the organoids exhibited the previously established phenotypic effects of the genetic manipulations (for instance, CRE organoids exhibited increased proliferation than control and shH19 organoids had reduced proliferation). The negative effect of Enzalutamide on murine organoids (**Figure 5b**) was surprising since we showed previously that H19 is modulated by AR signaling. We concluded that since murine organoids require DHT this system is not an ideal one to show the treatment with Enza. Alternatively, we decided to check for drug cytotoxicity in LNCaP cells.

LNCaP cells are androgen responsive and after TP53/RB1 knockdown become less sensitive to growth inhibition by AR antagonist ENZA than the parental cell line (3). However, when transduced with shH19 these prostate tumor cells regain sensitivity to hormone blockade (**Figure 5c**) and demonstrate growth inhibition by ENZA. Conversely, ENZA (2μM or 5μM) treatment for 5 days inhibited the growth of control LNCaP cells. *Together this data highlights the importance of H19 in regulating the sensitivity of prostate cancer cells to ADT.*

To investigate the role of PIM kinases in ADT, we analyzed the effect of Enza treatment on PIM1 overexpressing androgen-responsive PCa cell line LNCaP cells. For this, LNCaP cells were seeded into 96-well plates at a density of 5,000 cells per well and were allowed to grow under desired conditions. At the end of each experiment, cell viability was measured using XTT cell proliferation assay (Trevigen, Cat # 4891-025-K) following the manufacturer's protocol. Briefly, the XTT reagent was added to cell culture (1:2 dilution) and incubated for 4h at 37°C and 5% CO_2. The absorbance of the colored formazan product was measured at 450 nm. The results of this cell viability assay demonstrated that while Enza treatment (48h, 10μM) was cytotoxic to the empty vector transduced control LNCaP cells (EV), overexpression of PIM1 caused resistance to Enza treatment (**Figure 6a**). This result is consistent with our finding that PIM kinase activity stimulates increases in SOX2 (**Figure 4a**). To explore this further, we examined the growth of LNCaP with control vector transduction (LNCaP-EV) and H19 overexpression (LNCaP-H19), followed by treatment with increasing concentrations of PIM447 with or without Enza (2μM, 5μM) treatment for 72h (**Figure 6b, 6c**). The PIM inhibitor treatment significantly sensitized the control

LNCaP cells to growth inhibition by Enza (**Figure 6b**). Overexpression of H19 in LNCaP cells blocked the effect of PIM kinase inhibitor treatment (**Figure 6c**). Additionally, treatment of LNCaP cells (**Figure 6d**) with PIM inhibitor decreased H19 levels indicating that Pim inhibitor works through suppressing H19 to overcome Enza resistance.

These results suggest that the PIM-mediated control of H19 levels modulates Enza sentitivity in LNCaP cells. Overall, the experiments conducted for Specific Aim 2 Task 1 Year 1 demonstrate in vitro that the level of lncRNA H19 is responsible for Androgen deprivation therapy in cell culture and murine organoid models and inhibiting this axis will restore the sensitivity to Enza thereby treating this highly aggressive prostate tumor.

Specific Aim 2: Major task 4: Writing the manuscript(s) derived from results of the project

Under this task of writing manuscripts derived from the results of the project generated through this grant.

Through the experiments conducted in year 1 of the research supported by this grant, I have been able to prepare a manuscript as the first author presenting the results of the findings under the guidance with my mentor Dr. Andrew Kraft. The results shown are all conducted under in vitro conditions and the manuscript is titled “PIM protein kinases regulate the level of the long noncoding RNA H19 to control stem cell gene transcription and modulate tumor growth”. Please see Appendix B for a copy of the manuscript that has been submitted to Molecular oncology and is currently under consideration for publication in the journal.

Training specific tasks:

Major task 1, Year 1: Training and educational development in prostate cancer research

I am continuing to further my training and educational development in the field of prostate cancer research and have accomplished this task through the following.

Poster presentation (Subtask 4)

- Presented my research from this project at Association of American Cancer research (AACR) Annual meeting 2019, Atlanta, Georgia. The presentation was titled “Role of long noncoding RNA H19 in driving enzalutamide resistant neuroendocrine prostate cancer” and was published in Cancer Research as a conference paper (DOI: 10.1158/1538-7445.AM2019-3017 Published July 2019).

Oral presentation (Subtask 2/4)

- Invited Oral presentation at Prostate Cancer Working Group Annual Meeting: New Strategies for Lethal Disease held at University of Arizona Cancer center on June 19, 2019. Title of presentation: “Role of lncRNA H19 in Neuroendocrine Prostate Cancer”.

Workshops (Subtask 1)

- Attended the Organoid workshop at AACR Annual meeting 2019.
- Attended Personal development workshop at AACR annual meeting 2019.

While attending these conferences and workshops enhance my skills and understanding in the field of prostate cancer, I continue to attend weekly lab meetings and Journal club from our lab (Subtask 3) where I provide updates on my progress in Research. Also, I attend monthly PCa group meeting at the UACC to understand and be abreast of the PCa research going on at the department.

Plan for the next reporting period to accomplish the goals:

Research specific tasks:

I plan to accomplish completion of **Specific Aim 1 Major Task 5** which will be very crucial to elucidate the clear mechanism behind the signaling cascade identified in the year 1. This would include

- Bisulphite sequencing to examine changes in methylation levels at H19 promoter on Pim1 overexpression.
- Reduced Representation Bisulphite sequencing to examine changes in global methylation pattern on H19 knockdown upon the loss of P53/Rb in organoids.

- Chromatin immunoprecipitation (ChIP) will be performed to determine changes in CTCF binding to H19 in Pim-overexpressing organoids or p53/Rb deletion.

I plan to accomplish completion of **Specific Aim 2 Major Task 2 and 3** that underly the in vivo testing of the initially proposed and in vitro (year 1) tested therapeutic combination of small molecule inhibitor of PIM and H19 knockdown to overcome Enza resistance. These findings will be key as they will reveal whether the proposed combination therapy is potent under pre-clinical conditions. This would include:

- Evaluate whether Pim inhibitors can overcome Enza resistance in stem cell derived tumors in vivo
- Enhancing the activity of the Pim and enzalutamide targeted therapy

Training specific tasks:

I plan to continue presenting my research from this project in various meetings that would be helpful to generate collaborations for future projects. As I would be reaching the final year of the grant I plan to progress my career forward by planning additional manuscripts and projects derived out of this research. Attending an annual workshop in enhancing my skills and professional development will also be planned to accomplish. Overall, under guidance from my mentor, I would plan during this year to realize my long term goal of becoming an independent investigator in a research intensive institution.

References

1. Semenas J, Dizeyi N, Persson JL. Enzalutamide as a second generation antiandrogen for treatment of advanced prostate cancer. *Drug Des Devel Ther*. 2013;7:875–881. Published 2013 Aug 27. doi:10.2147/DDDT.S45703

2. Tucci M, Zichi C, Buttigliero C, Vignani F, Scagliotti GV, Di Maio M. Enzalutamide-resistant castration-resistant prostate cancer: challenges and solutions. *Onco Targets Ther*. 2018;11:7353–7368. Published 2018 Oct 24. doi:10.2147/OTT.S153764

3. Ku SY, Rosario S, Wang Y, et al. Rb1 and Trp53 cooperate to suppress prostate cancer lineage plasticity, metastasis, and antiandrogen resistance. *Science*. 2017;355(6320):78–83. doi:10.1126/science.aah4199

4. Mu P, Zhang Z, Benelli M, et al. SOX2 promotes lineage plasticity and antiandrogen resistance in TP53- and RB1-deficient prostate cancer. *Science*. 2017;355(6320):84–88. doi:10.1126/science.aah4307

5. Drost J, Karthaus WR, Gao D, et al. Organoid culture systems for prostate epithelial and cancer tissue. *Nat Protoc*. 2016;11(2):347–358. doi:10.1038/nprot.2016.006

6. Karthaus WR, Iaquinta PJ, Drost J, et al. Identification of multipotent luminal progenitor cells in human prostate organoid cultures. *Cell*. 2014;159(1):163–175. doi:10.1016/j.cell.2014.08.017

7. Berman-Booty LD, Knudsen KE. Models of neuroendocrine prostate cancer. *Endocr Relat Cancer*. 2015;22(1):R33–R49. doi:10.1530/ERC-14-0393

Supporting data

Figures 1-6

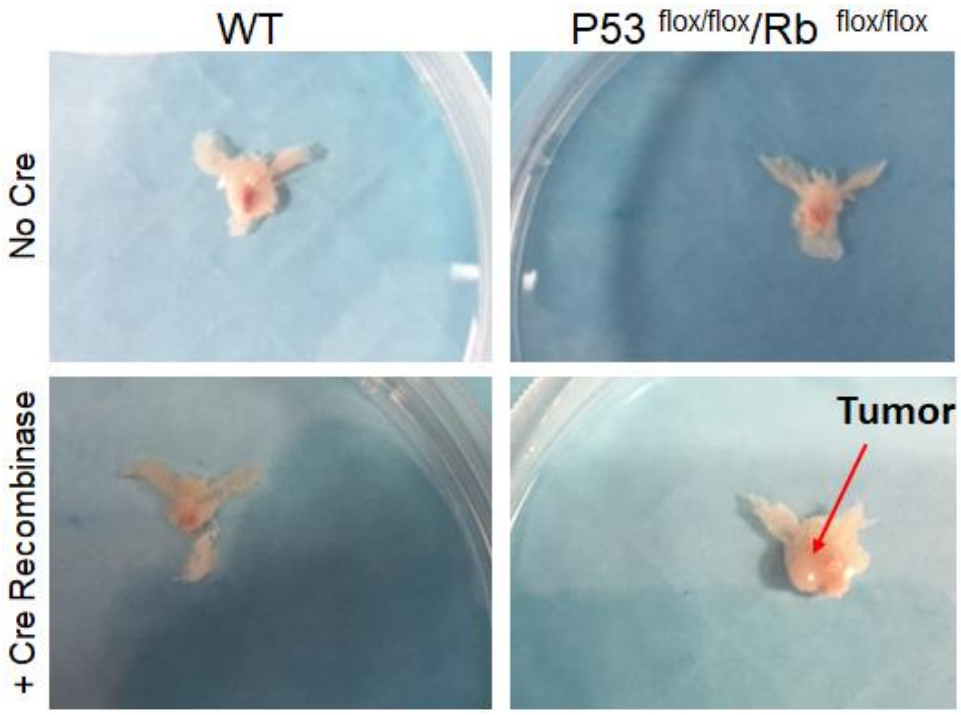

Figure 1a: Representative images of prostate tissue isolated from different mice as indicated. Note the Tumor development in the P53/Rb mouse induced to express Cre recombinase thus leading to a loss of P53/Rb. These prostate tissues were further dissociated to develop murine prostate organoids.

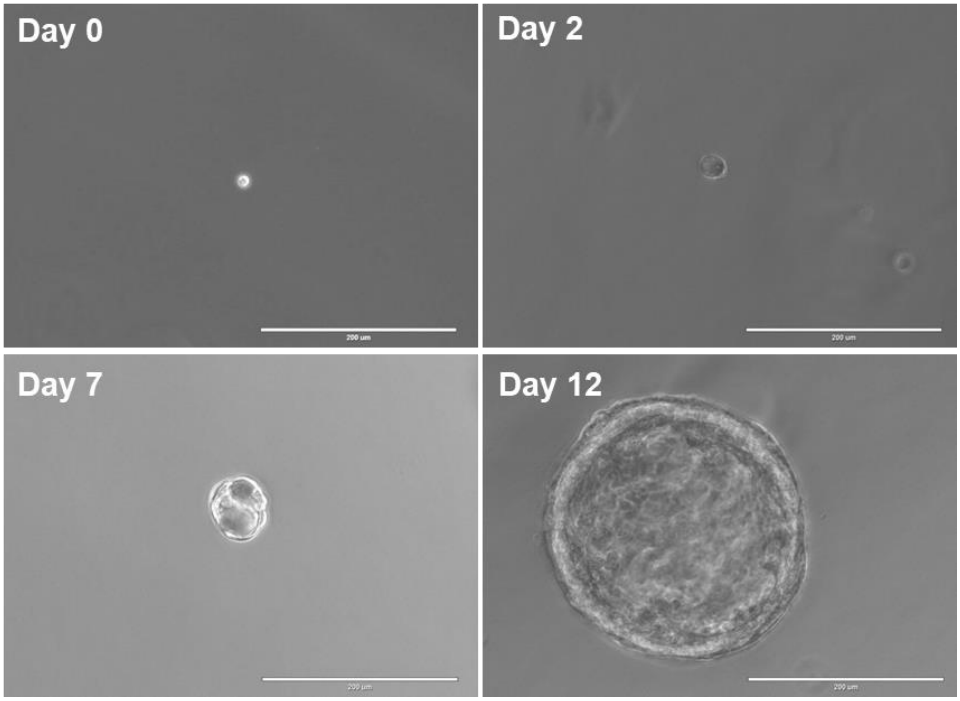

Figure 1b: Phase contrast images demonstrating progression of growth of a representative murine prostate organoid from a single cell. Scale bar: 200µm.

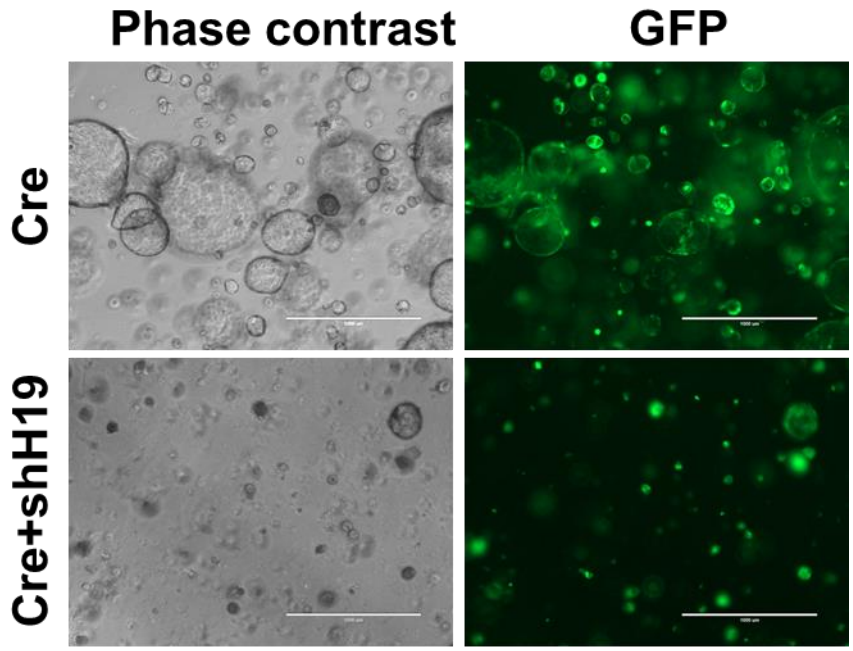

Figure 2a: Representative images of murine prostate organoids derived from P53 $^{flox/flox}$/RB $^{flox/flox}$. The organoid were then transduced with lentivirus expressing Cre recombinase (Cre) and another lentivirus expressing shRNA to H19 (shH19). Successful transductions are indicated by the GFP fluorescence due to lentiviral transduction. Scale bar: 1000μm.

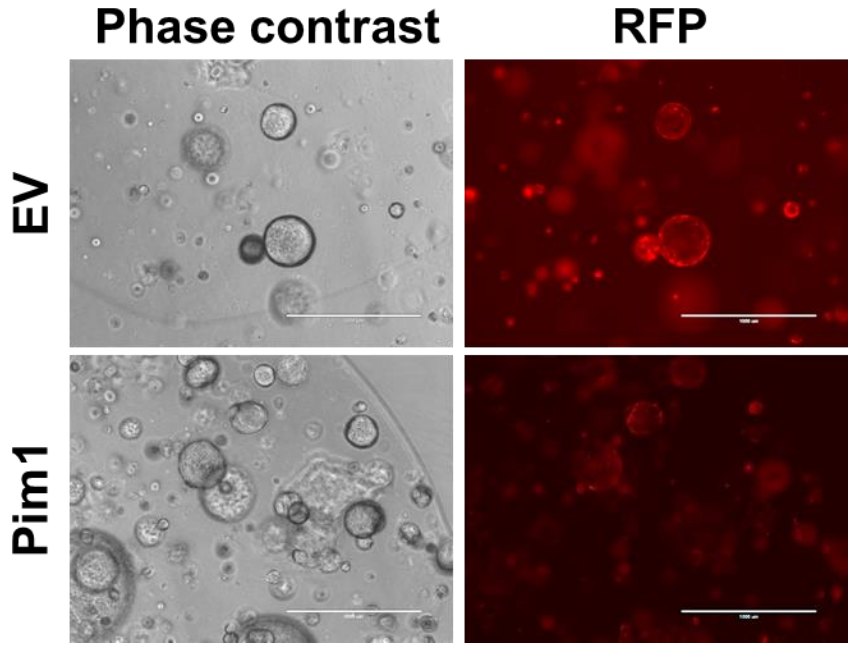

Figure 2b: Representative images of murine prostate organoids derived from Wild type mice. The organoid were then transduced with lentivirus overexpressing PIM1 (PIM1) and another lentivirus expressing empty vector used as a control (EV). Successful transductions are indicated by the RFP fluorescence due to lentiviral transduction. Scale bar: 1000μm.

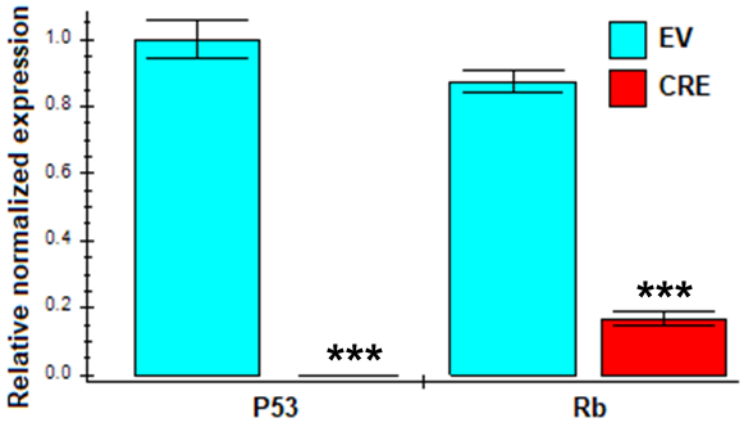

Figure 2c: Relative RNA expression indicating the loss of P53 and Rb in P53 $^{flox/flox}$/RB $^{flox/flox}$ murine prostate organoids transduced with lentivirus expressing Cre recombinase (CRE). The empty vector (EV) transduced organoid was used as a control. Values are mean +/- S.D. n=3, *** indicates p values<0.001.

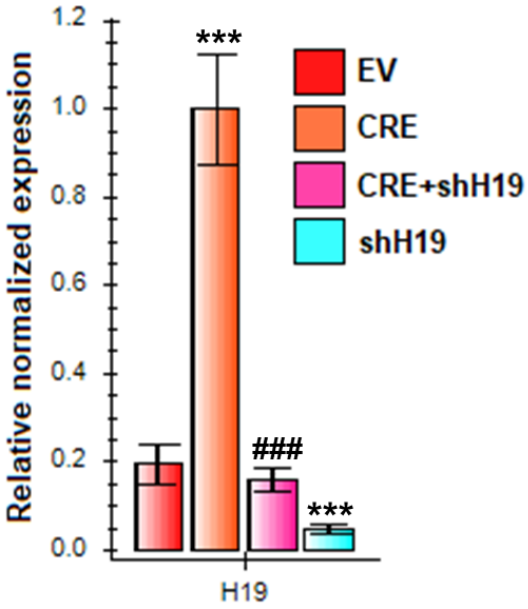

Figure 2d: Relative RNA expression indicating the knockdown of H19 in P53 $^{flox/flox}$/RB $^{flox/flox}$ murine prostate organoids both in control organoids (shH19) and CRE organoids (CRE+shH19) after lentiviral transduction with shH19. Positive controls include Cre recombinase (CRE) expressing organoids that show enhanced expression of H19.. The empty vector (EV) transduced organoid was used as a control. Values are mean +/- S.D. n=3, *** indicates p values<0.001 vs EV, ### indicates p values<0.001 vs CRE.

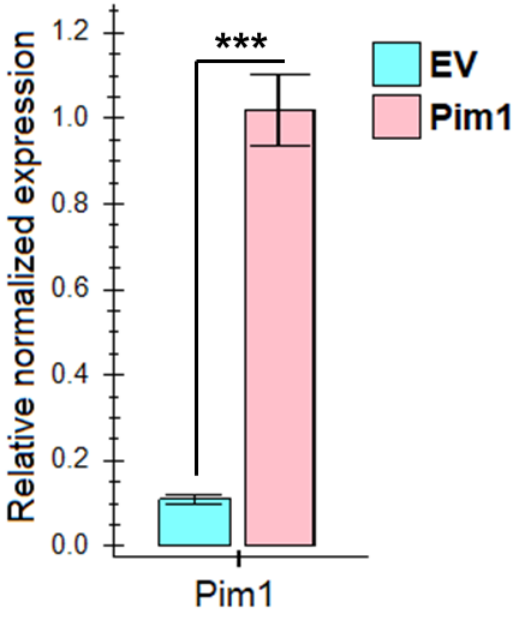

Figure 2e: Relative RNA expression indicating the overexpression of Pim1 in Wild type murine prostate organoids transduced with lentivirus expressing Pim1 (Pim1). The empty vector (EV) transduced organoid was used as a control. Values are mean +/- S.D. n=3, *** indicates p values<0.001.

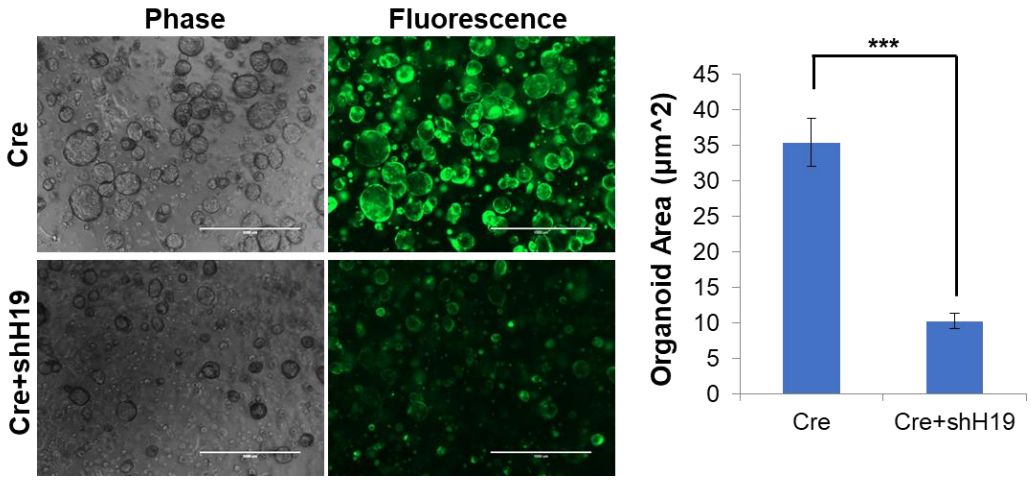

Figure 3a: Mouse organoid cells (5000/well/condition) were plated for organoid growth analysis. Right: Representative fluorescence images. Magnification: 4x, Scale bar: 1000µm, left: Organoid area quantification (n=10). Values are mean +/- S.D., n=3, ***p value<0.001.

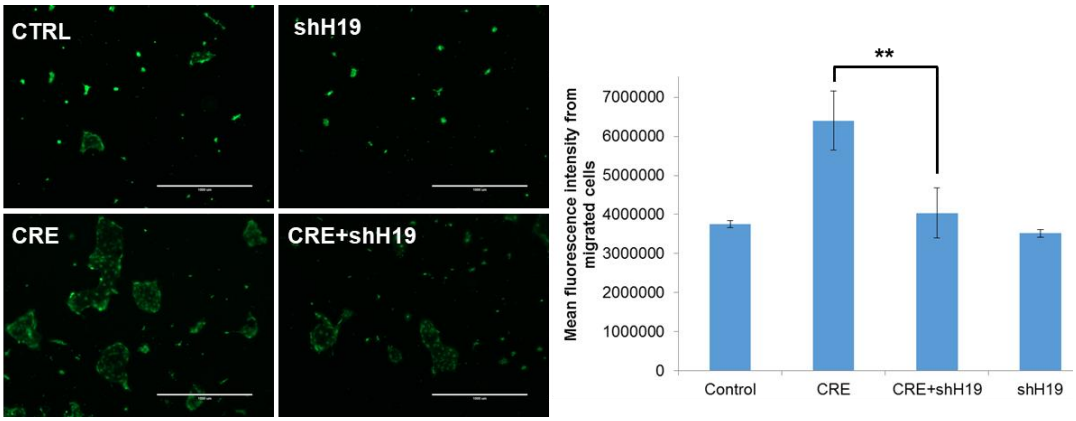

Figure 3b: Organoid invasion assay. Transwell assay using FluoroBlock inserts with 50,000 cells/well of DKO organoids transduced with a Control (CTRL), CRE and CRE+shH19 (n=3). fluorescence intensity of migrated cells on the bottom of the transwell was quantified 5 days post-plating. Ctrl-GFP was used as control. Values are mean +/- S.D., n=3, ***p value<0.001.

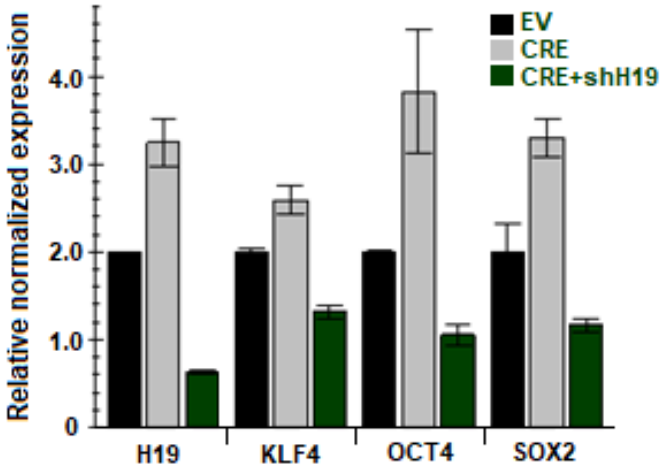

Figure 3c: Relative RNA expression of stem cell genes in mouse prostate organoids after P53/Rb1 double knockdown induced by lentiviral transduction of Cre-recombinase in $P53^{flox/flox}/Rb1^{flox/flox}$ mouse prostate organoids (Cre) and H19 knockdown (Cre+shH19). EV transduced organoids (EV) were used as controls. Values are mean +/- S.D. from 3 independent experiements.

Figure 3d: WB of representative stem cell genes in the *Trp53*$^{flox/flox}$/*Rb1*$^{flox/flox}$ mouse prostate organoids transduced with EV, Cre, Cre+shH19 or shH19.

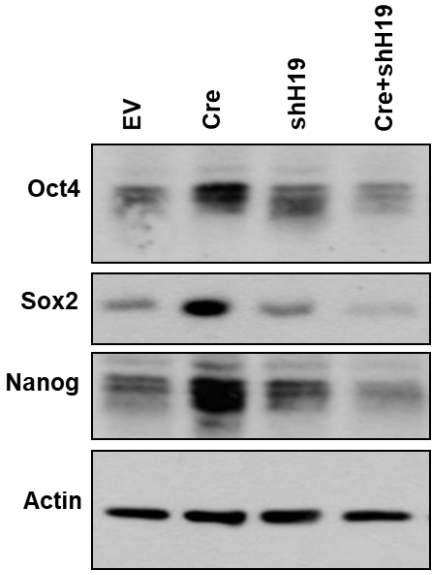

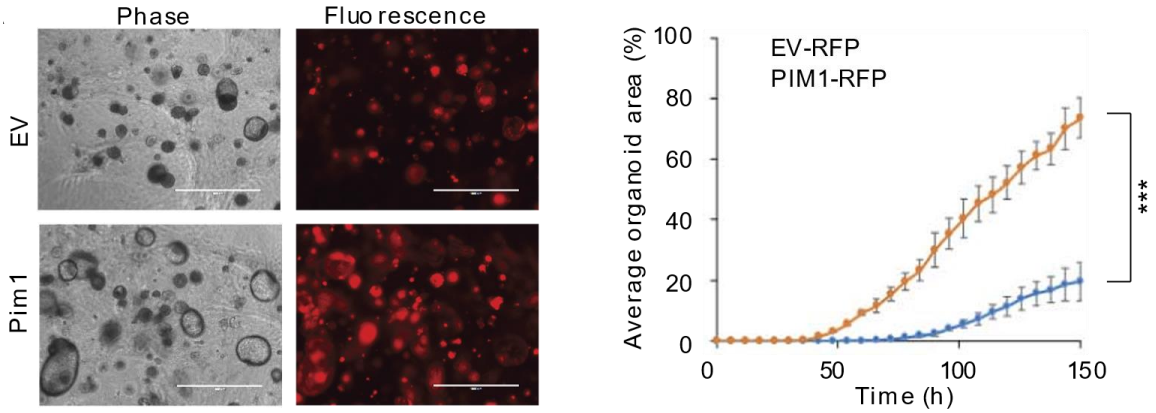

Figure 4a: Mouse prostate organoid cells transduced with empty vector (EV-RFP) or FUCRW-PIM1 plasmid (PIM1-RFP) (5000/well) were plated for organoid growth analysis. Representative images of the growth analysis (left panel), scale bar: 1000µm. Quantification of the organoid growth (right panel). Values are mean +/- SEM; n=6; ***p<0.001.

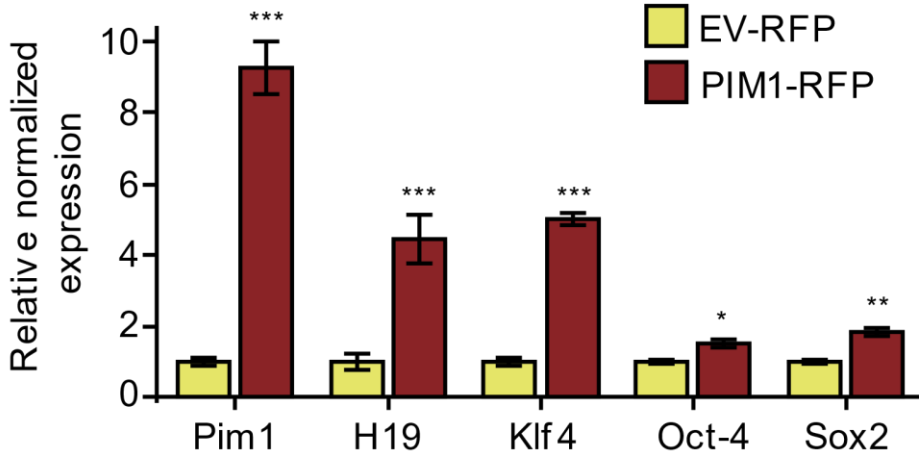

Figure 4b: Relative RNA levels of Pim1, Klf4, Oct-4, Sox2 in mouse prostate organoids described in A. RNA expression was normalized to Hprt RNA. Values are mean +/- SEM; n=3; *p<0.05, **p<0.01, ***p<0.001.

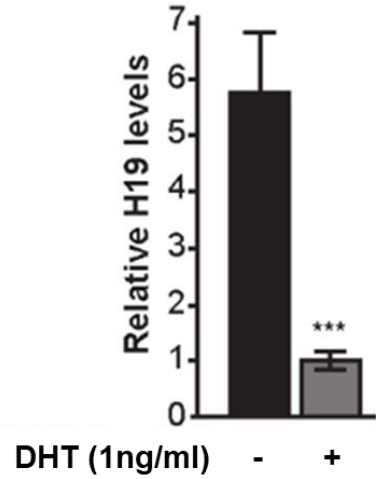

Figure 5a: Relative H19 expression in murine prostate organoids upon DHT removal from media (-) as compared to culture with regular media containing DHT Data are Mean+/- SEM, n=3. ***, p<0.001.

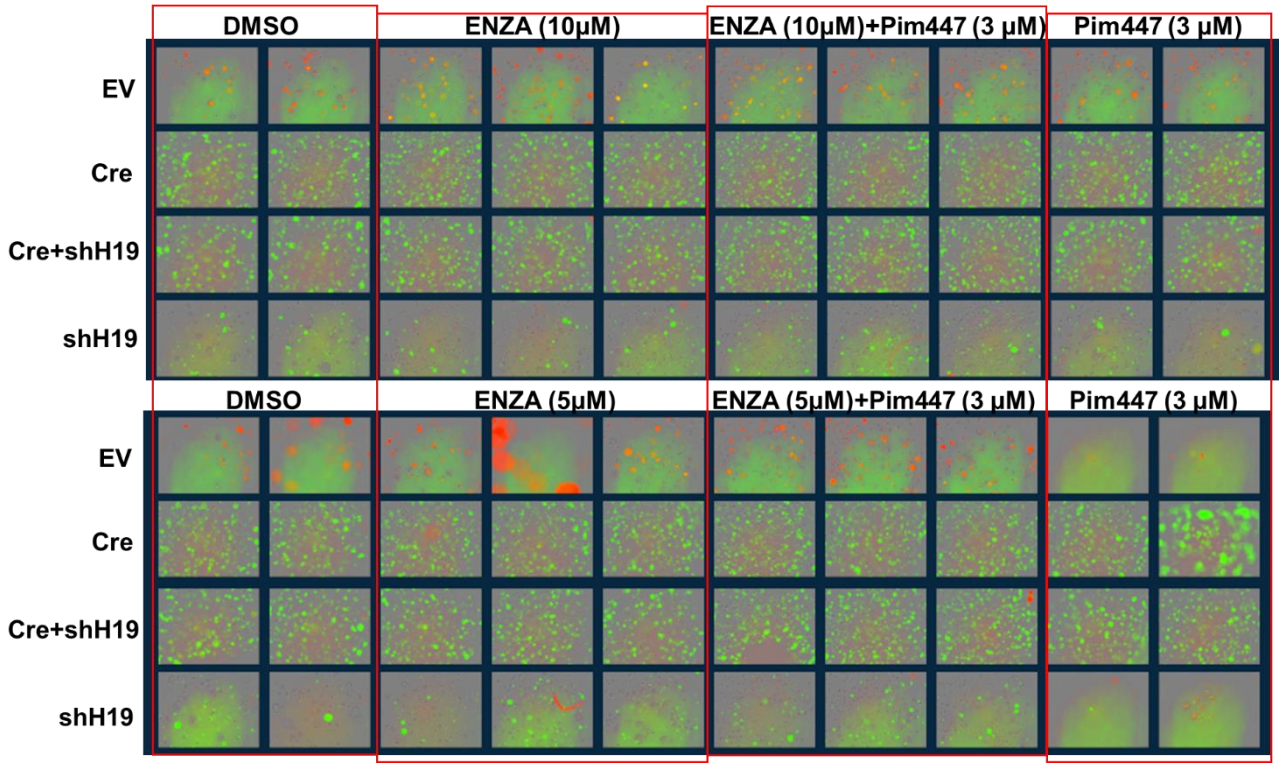

Figure 5b: Organoid growth assay as measured by a live cell imaging system. Organoids were dissociated with TrypLE (Invitrogen) into tiny cell clusters, plated (5000 cell clusters/well) and treated under desired conditions for 4-6 days. A real-time imaging system (Incucyte) was used to measure organoid growth. Images were captured every 12h. The images shown above are a compilation of Pim inhibitor and Enza treatment either individually or in combination (as seen on day 5) when added to Control EV and CRE organoids with or without H19 knockdown (shH19). As observed from the images of multiple replicates of the each treatment condition- Enza treatment did not appear to modulate organoid growth in this system.

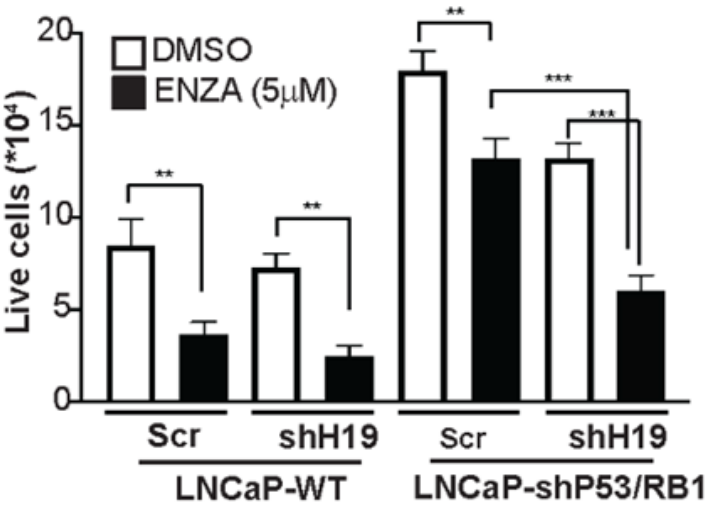

Figure 5c: Growth response of TP53/RB1 knockdown (shTP53/RB1) LNCaP with and without knockdown of H19 (shH19 vs Scr) exposed to 5 μmol/L of ENZA for 5 days. DMSO was used for control treatment.

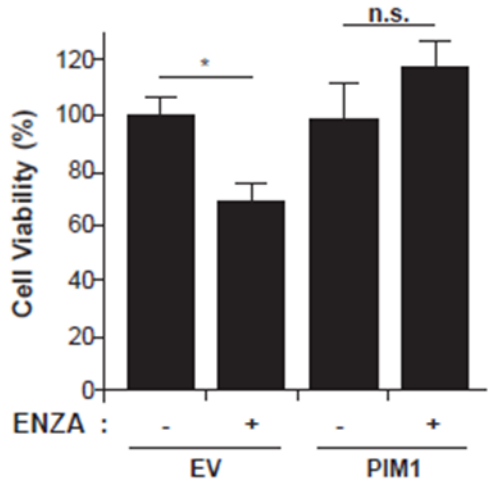

Figure 6a: Percent cell viability of LNCaP cells stably expressing empty vector (EV) or FUCRW-PIM1 plasmid (PIM1), treated with Enza (MDV3100, 10μM, 48h). DMSO treatment was used as control.

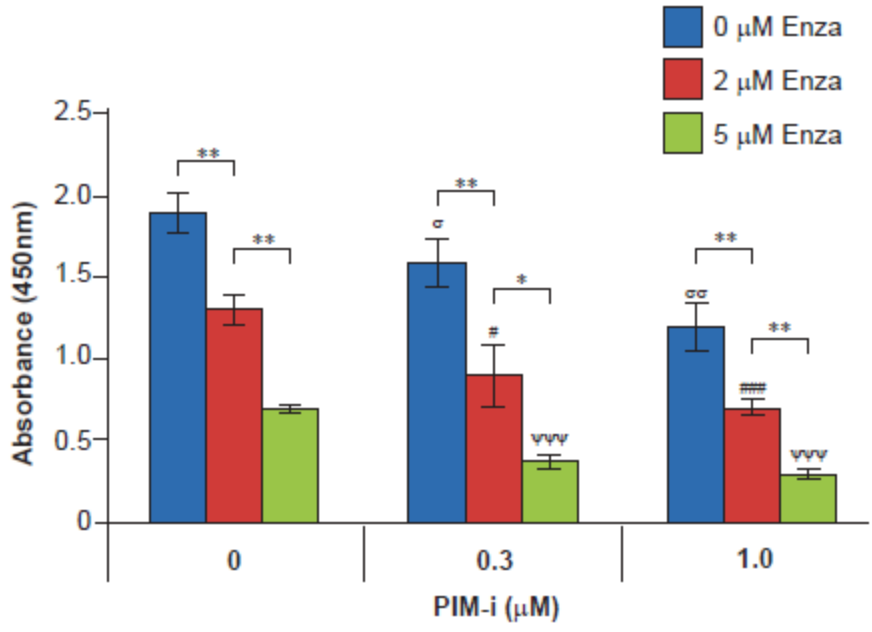

Figure 6b: Cell viability of LNCaP cells stably expressing empty vector (LNCaP-EV) treated with either Enza (2μM and 5μM) or PIM-i (0.01μM, 0.03μM, 0.1μM, 0.3μM and 1μM, 72h) and combination, measured by XTT assay. Treatment with 0μM denotes DMSO treatment in lieu of the inhibitor. Values are mean +/- SEM; n=3; *p<0.05, **p<0.01, ***p<0.001.

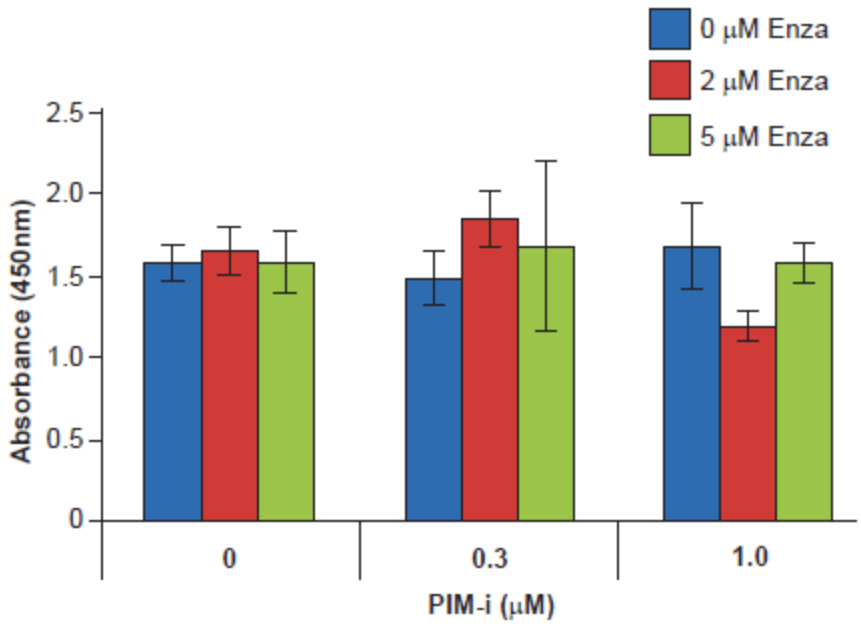

Figure 6c: Cell viability of LNCaP cells stably overexpressing H19 (LNCaP-H19) treated with Enza or PIM-i and combination, as stated in Fig. 6b. XTT assay was carried out 72h after the start of drug treatment and absorbance was measured at 450nm. Results from cell viability in Fig. 6b and 6c were represented as absorbance at 450nm. Values are mean +/- SEM; n=3.

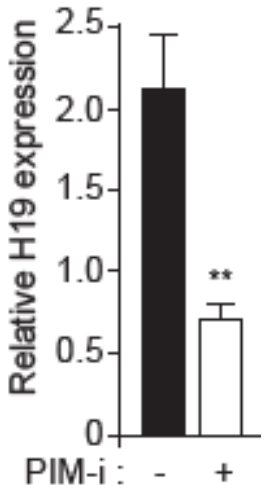

Figure 6d: Relative H19 RNA expression in LNCaP cells treated with PIM-i (PIM447, 1 µM, 24h). DMSO was used for control treatment. Relative H19 expression was normalized to 18S RNA. Values are mean +/- SEM; n=3; **p<0.01.

4. Impact

Prostate cancer remains the second largest killer of men with cancer in the United States. The commonly administered antiandrogen drug- Enzalutamide has been shown to be very effective in PCa patients. But, more and more patients are escaping or became unresponsive to this androgen deprivation therapy (ADT). The proposed research project investigates mechanistic details into the resistance to ADT specifically by enzalutamide and aims to identify the role of upregulated Pim1/H19/ Sox2 pathway in driving such resistance. The findings during year 1 from this study has identified the Pim/H19 as key players in mediating antiandrogen resistance (Manuscript under minor revision in "Molecular Oncology" journal- Appendix B). These results will help introducing and detecting novel pathways which have the potential to be targeted against resistance to ADT. Further experiments under in-vivo condition as proposed during Year 2 will help solidify the above pathway which could lead to the potential development of various different therapeutic combinations in future to effectively target advanced metastatic prostate cancer.

Secondly, results from the Year 1 of the study indicated that combination of pan-Pim kinase inhibitor and antiandrogen- Enzalutamide was shown to have synergistic effect in treatment of PCa cells. Studies proposed for year 2 will extrapolate these finding to in vivo conditions. The proposed therapeutic combination would be helpful in targeting patients with advanced stage of prostate cancer and stop them to progress the cancer in an event they develop resistance to an already clinically effective second generation drug.

Overall, the impactful outcomes of year 1 of this study are as follows:

- Identification of novel resistance mechanism pathway in the form of PIM/H19/SOX2 for ADT.
- Novel therapeutic combinations of PIM inhibitor and anti-androgen Enzalutamide to overcome the associated resistance in vitro.
- For training related goals – I was able to present my research at local and international meetings (Appendix A) and was able to prepare a manuscript as a first author highlighting the results from this project which is currently under review in the journal "Molecular Oncology" (Appendix B).

5. Changes/Problems

A minor issue in Specific aim 2 -Major task 1: The murine organoids treated with PIM1 inhibitor and Enza did not show any changes under in vitro conditions (**Figure 5b**). As I attended the organoid workshop at AACR 2019, I gained insights into this negative result where the organoid experts claimed that it has been shown that in-vitro treatment of organoids with various drugs

especially Enzalutamide will not show any changes mainly because the organoids require DHT which interferes with our experiment. This was not known at the time of designing the experiments. Alternatively, we performed the experiments in LNCaP cells, which are commonly used prostate cancer cell line that are androgen responsive. We note that the switch from murine organoids to LNCaP cells in some experiments is a minor change and does not alter either the scope or direction of the project.

6. Products

- Journal publication:

Singh N, Padi SKR, Bearss JJ, Pandey R, Okumura K, Beltran H, Song JH, Kraft AS, Olive V. PIM protein kinases regulate the level of the long noncoding RNA H19 to control stem cell gene transcription and modulate tumor growth. **Molecular Oncology.**
Manuscript ID- MOLONC-19-0875.R1
Status of publication - Under review. Revision submitted 01/09/2020).
Acknowledgement of federal support - Yes

- Conference paper:

Abstract of research presentation during the AACR Annual meeting, 2019 as published in Cancer Research 2019.

Neha Singh, Virginie Olive, Ritu Pandey, Jin Song, Jeremiah Bearrs, Sathish K. Padi, Koichi Okumura, Andrew S. Kraft. Role of long noncoding RNA H19 in driving enzalutamide resistant neuroendocrine prostate cancer [abstract]. In: Proceedings of the American Association for Cancer Research Annual Meeting 2019; 2019 Mar 29-Apr 3; Atlanta, GA. Philadelphia (PA): AACR; Cancer Res 2019;79(13 Suppl):Abstract nr 3017.

7. Participants & Other Collaborating Organizations

N/A

8. Special Reporting Requirements

N/A

9. Appendices

Attachments

- Appendix A: Abstract of research presentation during the AACR Annual meeting, 2019 as published in Cancer Research 2019.

Neha Singh, Virginie Olive, Ritu Pandey, Jin Song, Jeremiah Bearrs, Sathish K. Padi, Koichi Okumura, Andrew S. Kraft. Role of long noncoding RNA H19 in driving enzalutamide resistant neuroendocrine prostate cancer [abstract]. In: Proceedings of the American Association for Cancer Research Annual Meeting 2019; 2019 Mar 29-Apr 3; Atlanta, GA. Philadelphia (PA): AACR; Cancer Res 2019;79(13 Suppl):Abstract nr 3017.

- Appendix B: First author Manuscript “under review” in the journal “Molecular Oncology” generated through the efforts conducted with the help of this grant.

Singh N, Padi SKR, Bearss JJ, Pandey R, Okumura K, Beltran H, Song JH, Kraft AS, Olive V. PIM protein kinases regulate the level of the long noncoding RNA H19 to control stem cell gene transcription and modulate tumor growth. **Molecular Oncology.**
Manuscript ID- MOLONC-19-0875.R1

Appendix A

Abstract of research presentation during the AACR Annual meeting, 2019 as published in Cancer Research 2019.

Abstract 3017: Role of long noncoding RNA H19 in driving enzalutamide resistant neuroendocrine prostate cancer

Neha Singh, Virginie Olive, Ritu Pandey, Jin Song, Jeremiah Bearrs, Sathish K. Padi, Koichi Okumura and Andrew S. Kraft

DOI: 10.1158/1538-7445.AM2019-3017 Published July 2019

Proceedings: AACR Annual Meeting 2019; March 29-April 3, 2019; Atlanta, GA

Abstract

INTRODUCTION: Approximately one-fourth of the prostate cancer (PCa) patients relapsing androgen deprivation therapy (ADT) have been shown to develop neuroendocrine prostate cancer (NEPC). One of the primary mechanisms attributed to this resistance is the lineage switching of epithelial cells to neuroendocrine (NE) phenotype making them independent of androgen receptor (AR) pathways for survival. Molecular basis essential to this lineage switch requires further elucidation. Thus, we aim to understand key mechanistic pathways that drive the development and maintenance of NEPC, and to investigate if the inhibition of pathway can re-sensitize to ADT in NEPC.

METHODS: Bioinformatics analysis was performed with existing databases to compare prostate adenocarcinoma (PCA) vs NEPC. Molecular features of NEPC have been shown to depict RB1 loss in 70-90% and TP53 loss in 56-67% of the cases. Thus, we established prostate organoid cultures from $P53^{fl/fl}$/$Rb^{fl/fl}$ mouse and infected them with Cre-lentivirus for combined loss of TP53/Rb1. Various PCA and NEPC cell lines and patient derived organoids were used to study the role of the long non-coding RNA H19 in NEPC. Organoid growth were assessed with Incucyte and invasive capacity was measured by Matrigel invasion assay.
RESULTS: Bioinformatic analysis of exisiting human PCa data sets demonstrate that H19 is one of the most highly expressed genes in NEPC and parallels the expression of NE markers. Indeed, we confirmed that H19 expression was high in various NEPC cell lines and NE patient derived organoids. H19 was also found to be markedly induced in mouse prostate organoids and LNCaP cells after TP53/Rb1 loss. Importantly, overexpression of H19 induced NE genes while suppressing the genes involved in AR signaling in LNCaP and primary PCa patient derived organoids and inversely, knockdown (KD) of H19 in LNCaP and mouse prostate organoids with TP53/Rb1 loss reduced the expression of NE gene. Interestingly, the KD of H19 in these cells re-induced the luminal phenotype, consequently restoring their sensitivity to ADT. These findings strongly implicate H19 in driving the NE lineage switch. The KD of H19 in these organoids led to a regression of tumor growth and invasiveness, suggesting H19 is required in malignant states. H19 KD decreases stem cell genes (SOX2, OCT4) via methylation of their promoters, and levels of EZH2, which methylates 'Lys-9' (H3K9me) and 'Lys-27' (H3K27me) of histone H3 and represses transcription of the target genes. H3K27me3 levels, which are high in NEPC, was reduced in the H19 KD, suggesting H19 works in an epigenetic regulation to induce NEPC phenotype.

CONCLUSION: These data highlight H19 as a novel regulator in controlling the lineage switch to NEPC, tumor growth, and the sensitivity to hormone blockade, suggesting that H19 regulation will be important for developing treatments specifically aimed for this highly aggressive form of prostate cancer.

Appendix B

First author Manuscript “under review” in the journal “Molecular Oncology” generated through the efforts conducted with the help of this grant.

Singh N, Padi SKR, Bearss JJ, Pandey R, Okumura K, Beltran H, Song JH, Kraft AS, Olive V. PIM protein kinases regulate the level of the long noncoding RNA H19 to control stem cell gene transcription and modulate tumor growth. **Molecular Oncology.**

Manuscript ID- MOLONC-19-0875.R1

PIM protein kinases regulate the level of the long noncoding RNA H19 to control stem cell gene transcription and modulate tumor growth

Neha Singh[1], Sathish K.R. Padi[1], Jeremiah J. Bearss[1], Ritu Pandey[1,2], Koichi Okumura[1,3], Himisha Beltran[4], Jin H. Song[1,2], Andrew S. Kraft[1,5*], Virginie Olive[1*]

[1]University of Arizona Cancer Center, University of Arizona, 1515 N. Campbell Ave. Tucson, AZ, USA 85724

[2]Department of Cellular and Molecular Medicine, University of Arizona, 1515 N Campbell Avenue, Tucson, AZ, USA 85724

[3]Department of Physiology, University of Arizona, 1515 N Campbell Avenue, Tucson, AZ 85724

[4]Department of Medical Oncology, Dana-Farber Cancer Institute, 44 Binney St, Boston MA 02115

[5]Department of Medicine, University of Arizona, 1515 N Campbell Avenue, Tucson, AZ, USA 85724

***Corresponding authors**

Andrew S. Kraft, M.D.
1515 N. Campbell Ave.
Tucson, Arizona 85724
Tel. 520-626-3425
akraft@uacc.arizona.edu

Virginie Olive, PhD
1515 N. Campbell Ave.
Tucson, Arizona 85724
Tel. 510-219-4012
v.olive@outlook.com

Running title: PIM regulates lncRNAH19 to drive stem cell genes

Key words: Pim kinase, H19, SOX2, T-ALL, prostate cancer, androgen deprivation therapy resistance.

ABSTRACT

The PIM serine/threonine kinases have an oncogenic and pro-survival role in hematological and solid cancers. However, the mechanism by which these kinases drive tumor growth has not been completely elucidated. To determine the genes controlled by this protein kinase we carried out a microarray analysis in T-cell acute lymphoblastic leukemia (T-ALL) comparing early progenitor (ETP-ALL) cell lines whose growth is driven by PIM kinases to more mature T-ALL that has low PIM levels. This analysis demonstrated that the long noncoding RNA (lncRNA) H19 was associated with increased PIM levels in ETP-ALL. Overexpression or knockdown of PIM in these T-ALL cell lines controlled the level of H19 and regulated the methylation of the H19 promoter, suggesting a mechanism by which PIM controls H19 transcription. In these T-ALL cells the expression of PIM1 induced stem cell gene expression (SOX2, OCT-4, NANOG) through H19. Identical results were found in prostate cancer cell lines where PIM kinases drive cancer growth, and both H19 and stem cell gene levels. Small molecule pan-PIM inhibitors currently in clinical trials reduced H19 expression in both of these tumor types. Importantly, the knockdown of H19 blocks the ability of PIM to induce stem cell genes in T-ALL cells, suggesting a novel signal transduction cascade. In prostate cancer, increases in SOX2 levels have been shown to cause both resistance to the androgen deprivation therapy (ADT) and the induction of neuroendocrine prostate cancer, a highly metastatic form of this disease. Treatment of prostate cancer cells with a small molecule pan-PIM inhibitor reduces stem cell gene transcription and enhances ADT. While overexpression of H19 blocks the ability of pan-PIM inhibitors to regulate hormone blockade. Together these results demonstrate that the PIM kinases control the level of lncRNA H19 which in turn modifies stem cell gene transcription regulating tumor growth.

1 INTRODUCTION

The PIM (Proviral Integration site for Moloney murine leukemia virus) protein kinase family, comprising three serine threonine protein kinases, PIM 1, 2, and 3, has been implicated in cancer initiation and progression (Brault et al., 2010; Cuypers et al., 1984). PIM kinases are elevated in hematopoietic neoplasms including myeloid leukemia, myeloma, and lymphoma (Alizadeh et al., 2000; Cohen et al., 2004; Wingett et al., 1996), and play an important role in prostate tumorigenesis (Chen et al., 2005; Shah et al., 2008). These enzymes have been associated with aggressive prostate tumor growth (Cibull et al., 2006). PIM kinases control tumor cellular metabolism, protein translation, cell growth and division, and play a clear role in the resistance to PI3K/AKT directed therapies in breast and prostate cancer (PCa) (Song et al., 2018). However, the specific targets and pathways that are regulated by the PIM kinases to drive cancer growth and progression have not been fully elucidated.

A stem cell gene expression signature has been shown to characterize poorly differentiated tumors from several types of human cancer (Ben-Porath et al., 2008). Tumor initiating cells expressing pluripotency factors, such as NANOG, OCT-4, and SOX2, play a significant role in the induction and maintenance of malignancy. Immortalized PCa epithelial cell cultures and DU145 human prostatosphere cells have been shown to express these stem cell genes (Gu et al., 2007; Rybak et al., 2011) which are enriched in high Gleason grade PCa (Mathieu et al., 2011) and predict the poorest overall survival (Markert et al., 2011). PIM1 transcriptional levels in embryonic stem (ES) cells are controlled by STAT3 and leukemia-inhibitory factor which are known to regulate stem cell genes (Aksoy et al., 2007). When ES cells are fused to fibroblasts, the addition of IL-6 to stimulate these cultures upregulates PIM1 levels which then cooperates with OCT-4, SOX2 and KLF4 to increase induced pluripotent stem cell frequency (Brady et al., 2013). Consistent with a role in stem cells, transgenic mice overexpressing PIM1 upregulate hematopoietic stem/progenitor cell proliferation, while PIM1 knockout mice have impaired long-term hematopoietic repopulating capacity (An et al., 2013). Together these findings suggest that the PIM kinases could regulate stem cell genes to control cancer growth.

We demonstrate that the PIM1 protein kinase induces the long noncoding RNA (lncRNA) H19 expression and promotes induction of a stem cell signature in both T-cell acute lymphoblastic leukemia (T-ALL) and PCa cells. The lncRNA H19 is highly expressed in embryonic tissue and placenta and repressed after birth (Pachnis et al., 1988; Poirier et al., 1991), but is highly re-expressed in multiple cancers including both hematopoietic (Takeuchi et al., 2007) and solid tumors including breast (Adriaenssens et al., 1998), esophageal (Hibi et al., 1996), bladder (Ariel

et al., 1995; Elkin et al., 1995), lung (Kondo et al., 1995), endometrial and cervical (Lee et al., 2003). H19 is encoded by the IGF2/H19 imprinted gene cluster located on human chromosome 11p15 (Zemel et al., 1992), and its transcription is controlled by differentially methylated regions (DMRs) of the upstream DNA called “imprinting control regions” (ICR). When hypomethylated, four specific DMRs upstream of H19 start site bind the transcription factor CTCF which acts as insulator preventing IGF2 promoter activation and enhancing H19 transcription (Phillips and Corces, 2009). Here we show that PIM1 induces epigenetic changes in DNA methylation in the control regions of H19, suggesting a mechanism by which it regulates the transcription of this lncRNA. The inhibition of pan-PIM kinase activity and the knockdown of H19 sensitizes PCa cells to treatment with anti-androgen enzalutamide (Enza). In PCa and its highly aggressive variant neuroendocrine prostate cancer (NEPC) (Davies et al., 2018), which expresses elevated H19 levels as compared to adenocarcinoma (Ramnarine et al., 2018), the combination of pan-PIM kinase inhibitors with concomitant H19 knockdown reduces tumor growth. These results delineate a unique signaling cascade driven by the PIM kinases that involves a lncRNA and stem cell genes to regulate tumor growth.

2 MATERIALS AND METHODS

2.1 Cell culture

PC3, LNCaP and DU145 were purchased from the American Type Culture Collection (ATCC); PC3-LN4 and human prostate fibroblast cell line BHPrS1 (Zemskova et al., 2015), were cultured in RPMI supplemented with 2mmol/L Glutamax (Life Technologies) and 10% fetal bovine serum (FBS) (BioAbChem) at 37°C under 5% CO_2 as reported previously. The T-ALL cell lines HSB-2, DU.528, KOPT-K1, CUTLL1, HPB-ALL, and SUP-T1 (Padi et al., 2017) were cultured in RPMI-1640 supplemented with 2mM Glutamax (Life Technologies), 10% FBS (BioAbChem) at 37˚C under 5% CO_2. LASCPC-01 (ATCC) were grown in HITES media containing RPMI, 5% FBS, 10nM hydrocortisone, 10nM beta-estradiol (Sigma), insulin-transferrin-selenium (Life Technologies) and Glutamax (Life Technologies). hPrEC and mPrEC cells were cultured as described previously (Song et al., 2018). Phoenix-Eco cells (a gift from Dr. Jonathan Schatz, University of Miami Health System) and Fibrosarcoma cell line FLYRD18/mCAT-IRES-Bleo (a gift from Dr. Hans-Guido Wendel, Memorial Sloan Kettering Cancer Center) were cultured in DMEM + 2mM Glutamine + 10% FBS. All cell lines were maintained for no more than 6 months in culture and were routinely tested for Mycoplasma.

2.2 Organoid culture

The NEPC patient derived organoids OWCM-155 were provided by Dr. Himisha Beltran and were cultured as previously described (Puca et al., 2018). For murine organoids, cells were dissociated from the wild type mouse prostate and cultured as organoids as described (Drost et al., 2016). All studies involving the use of animals were approved by and conducted in accordance with the guidelines of the Institutional Animal Care and Use Committees at the University of Arizona Cancer Center. Both NEPC and murine organoids was replenished with fresh media every 3−4 days during organoid growth. Dense cultures with organoids ranging in size from 200 to 500μM were passaged weekly. Organoid cultures were bio-banked using Bambanker (Gibco) at −80°C.

2.3 RNA extraction, qPCR and gene expression analysis

Total RNA was isolated from cells using TRIzol reagent (Invitrogen, 15596–018). 1μg total RNA were reverse transcribed by using i-Script cDNA Synthesis System kit (Biorad, 1708891). To measure gene expression, Real time PCR was performed using SsoAdvanced™ Universal SYBR® Green Supermix (Biorad, 1725271), following the manufacturer's protocol. Expression level of each transcript was quantified by using Bio-Rad CFX96 Real-Time PCR Detection

System. Quantitative real-time PCR (qPCR) assay were performed using the following primers (5'-3'):

h-H19-F: GCACCTTGGACATCTGGAGT ,
h-H19-R: TTCTTTCCAGCCCTAGCTCA ; primer for H19 was designed based on Ref seq ID NR_002196.2. Amplicon length : 171

h-KLF4-F: GGCACTACCGTAAACACACG,
h-KLF4-R: CTGGCAGTGTGGGTCATATC; Amplicon length: 140

h-NANOG-F: TTTGTGGGCCTGAAGAAAACT,
h-NANOG-R: AGGGCTGTCCTGAATAAGCAG; Amplicon length: 116

h-OCT-4-F: TCGAGAACCGAGTGAGAGG,
h-OCT-4-R: GAACCACACTCGGACCACA; Amplicon length: 125

h-SOX2-F: CCCTGTGGTTACCTCTTCCT,
h-SOX2-R: AGTGCTGGGACATGTGAAGT; Amplicon length: 136

h-PIM1-F: CGACATCAAGGACGAAAACATC,
h-PIM1-R: ACTCTGGAGGGCTATACACTC; Amplicon length: 137

h-PIM2-F: GAACATCCTGATAGACCTACGC,
h-PIM2-R: CATGGTACTGGTGTCGAGAG; Amplicon length: 142

h-PIM3-F: GACATCCCCTTCGAGCAG,
h-PIM3-R: ATGGGCCGCAATCTGATC; Amplicon length: 147

h-cMYC-F: AAACACAAACTTGAACAGCTAC,
h-cMYC-R: ATTTGAGGCAGTTTACATTATGG; Amplicon length: 188

h-18S-F: GTAACCCGTTGAACCCCATT,
h-18S—R: CCATCCAATCGGTAGTAGCG; Amplicon length: 151

m-PIM1-F: GATCATCAAGGGCCAAGTGT,
m-PIM1-R: GATGGTTCCGGATTTCTTCA; Amplicon length: 122

m-OCT-4-F: TCAGGTTGGACTGGGCCTAGT,
m-OCT-4-R: GGAGGTTCCCTCTGAGTTGCTT; Amplicon length: 100

m-SOX2-F: GGTTACCTCTTCCTCCCACTCCAG,
m-SOX2-R: TCACATGTGCGACAGGGGCAG; Amplicon length: 193

m-KLF4-F: CCAAAGAGGGGAAGAAGGTCG,
m-KLF4-R: GTGCCTGGTCAGTTCATCGG; Amplicon length: 198

m-HPRT-F: AAGCTTGCTGGTGAAAAGGA,
m-HPRT-R: TTGCGCTCATCTTAGGCTTT. Amplicon length: 186

2.4 Immunoblotting

At the end of each experiment, cells were lysed in RIPA buffer (Cell Signaling Cat# 9806S) with complete protease/phosphatase inhibitor cocktail (Cell Signaling Cat# 5872S). The protein

concentration was determined by Bio-Rad DC protein assay (Bio-Rad). Western blots were performed as described previously (Song et al., 2018). The levels of PIM1 kinase (relative to ACTIN) and p-IRS1 (S1101) proteins (relative to IRS1) were quantified and normalized to their respective control samples using ImageJ software.

2.5 Antibodies and Reagents

Primary antibodies used for Western blotting included anti-PIM1 (Cell signaling technologies, Cat # 2907), anti-PIM2 (Cell signaling technologies, Cat # 4730), anti-PIM3 (Cell signaling technologies, Cat # 4165), anti-pIRS1-S1101 (Cell signaling technologies, Cat # S1101 Cat # 2385), anti-IRS1 (Cell signaling technologies, Cat # 06-248), anti-HA (Cell signaling technologies, Cat # 14031), anti-SOX2 ((E-4) sc-365823, Santa Cruz Biotech), anti-OCT-4 ((C-10) sc-5279, Santa Cruz Biotech), anti-NANOG ((5A10) sc-134218, Santa Cruz Biotech). HRP conjugated anti-β-actin (Cat # A3854) was purchased from Sigma. HRP-linked mouse IgG (Cat # NA931V) and rabbit IgG (Cat # NAV934V) were purchased from GE Healthcare Life Sciences.

Doxycycline (DOX) hydrochloride (Cat # D3447) was purchased from Sigma. AZD1208 (Cat # A13203) was purchased from Adooq bioscience. Enzalutamide (MDV3100) (Cat # S1250) was purchased from Selleckchem. PIM447 was a gift from Novartis.

2.6 Plasmids

Knockdown of human H19 was performed using the lentiviral plasmids pLenti-siH19-GFP (Abm, #i009382) and pLenti-scrambled siRNA-GFP (Abm, #LV015-G) as a control. These siH19 plasmids allow for direct non-viral plasmid transfection for immediate expression (siH19) and also package into lentiviral particles for high efficiency transduction and stably integrated expression (shH19). Overexpression of human H19 was performed using pLenti-GIII-CMV-H19-GFP-2A-Puro (Abm, # LV178008). The PIM1-expressing constructs as well as its K67M kinase-dead mutants were described previously (Cen et al., 2010). All the PIM1, 2 and 3 overexpression plasmids and siRNA to PIM1 were as previously described (Padi et al., 2017; Song et al., 2018). Transient transfection of siRNA and cDNA was performed using Lipofectamine 3000 (Invitrogen) and Xfect transfection reagent (Clontech). The SUP-T1 cells were engineered (SUP-T1E) using a fibrosarcoma cell line FLYRD18/mCAT-IRES-B (Ngo et al., 2006) and infected with MigR1 and MigPIM1 following established procedures (Peters et al., 2016).

2.7 Cell viability assay

LNCaP and PC3 cell lines were seeded into 96-well plates at a density of 5,000 cells per well and were allowed to grow under desired conditions. At the end of each experiment, cell viability was

measured using XTT cell proliferation assay (Trevigen, Cat # 4891-025-K) following the manufacturer's protocol. Briefly, the XTT reagent was added to cell culture (1:2 dilution) and incubated for 4h at 37°C and 5% CO_2. The absorbance of the colored formazan product was measured at 450 nm.

2.8 Organoid growth assay

Organoids were dissociated with TrypLE (Invitrogen) into tiny cell clusters, plated (5000 cell clusters/well) and treated under desired conditions for 4-6 days. A real-time imaging system (IncuCyte™, Essen Bio) was used to measure organoid growth. Images were captured every 12h and results were plotted as the percent average organoid growth versus time.

2.9 Luciferase assay

PC3 cells stably overexpressing Doxycyclin (DOX) inducible PIM1 (PC3 Tripz-PIM1), were plated in 96-well plates (2×10^4 cells/ well) and transfected with a OCT-4 (proximal and distal enhancer) luciferase reporters (Addgene) or Renilla (Promega) using Lipofectamine (Invitrogen). The plasmid sequences for OCT-4 distal and proximal enhancers were pGL3-human OCT-4 DE-SV40-Luc and pGL3-human OCT-4 PE-SV40-Luc and were a gift from Dr. Jacob Hanna (Addgene plasmid # 52414 and 52415 respectively) (Gafni et al., 2013). The total plasmid DNA used was normalized to 0.5µg per well by the addition of Renilla. At 24h after transfection, luciferase activities were measured using a Dual-Luciferase Reporter Assay System (Promega) and a GloMax 96 well microplate luminometer (Promega). OCT-4 (proximal and distal promoter) luciferase activities were corrected by the corresponding Renilla luciferase activities. Results are expressed in arbitrary light units.

2.10 Lentiviral Production and transduction

Lentiviral particle production and infection was performed as described previously (Tiscornia et al., 2006). For infection of adherent PCa cells, 10^6 cells/well were seeded in six-well plates and infected with concentrated lentiviral particles 1 day after seeding. For lentiviral transduction, organoids were pre-incubated for at least 48h with regular organoid media supplemented with Wnt-3a and Rho kinase inhibitor (Karthaus et al., 2014). After 48h, organoids were dissociated with TrypLE and spinoculated with lentiviral particles along with polybrene (8µM final concentration) at 600g for 1h at 32°C. After incubating organoid cells at 37°C for 3h, the cells were replated in Matrigel in ENR media without lentivirus and allowed to grow for several days.

2.11 Bisulfite sequencing

Genomic DNA from informative samples were treated with bisulfite (EpiTect Plus DNA Bisulfite Kit, Qiagen, Cat No./ID: 59124) to convert unmethylated cytosines to uracils whereas methylated cytosines are unaffected according to manufacturer's protocol. Bisulfite-treated DNA was subsequently amplified using the forward 5′-TGGGTATTTTTGGAGGTTTTTTT-3′ and reverse primer 5′- TCCCATAAATATCCTATTCCCA 3′.

2.12 Fluorescent activated cell sorting

Cells were resuspended in 10% FBS/phosphate-buffered saline (PBS) to reach a concentration of 10^7 cells per milliliter. Twenty microliters of the cell suspension were stained with various antibodies diluted in 10% FBS/PBS for 1h. Subsequently, cells were washed with 2% FBS/PBS and resuspended in 10% FBS/PBS for flow cytometry analysis (FACS). Antibodies used for our FACS analyses include APC anti-human CD24 antibody (#311117, Biolegend), PE anti-human CD29 antibody (#303003, Biolegend), APC anti-Human CD133 (Cat. No.17-1338-41, eBioscience) and APC anti-Human CD49b (Integrin alpha 2) (Cat. No.17-0500-41, eBioscience).

2.13 Affymetrix gene chip expression analysis

Total RNA was extracted from six T-ALL cell lines using the RNAeasy kit following manufacturer's instructions (QIAGEN Cat #74104). The Genomics Facility Core at University of Arizona Cancer Center performed quality control using the Agilent Bioanalyzer 2100 to confirm all RNA samples had RNA Integrity Numbers (RINs) greater than seven and to quantitate the concentration. From the RNA, the Genomics Core produced labeled a DNA target using the WT PLUS reagent kit and hybridized it to the Affymetrix® HTA 2.0 Array overnight according to the manufacturer's instructions. Arrays were washed and scanned with the GeneChip Hybridization Wash and Stain kit and an Affymetrix® Scanner 3000 following the manufacturer's instructions. The Affymetrix® Transcriptome Analysis Console v3.0 software was used to analyze resulting data file to identify differentially expressed genes between PIM-i sensitive cells (HSB-2, DU.528, and KOPT-K1) and PIM-i insensitive cells (CUTLL1, HPB-ALL, and SUP-T1) and generated a scatter-plot of differentially expressed genes with the following criteria: Fold Change (linear) < - 2 or Fold Change (linear) > + 2 and ANOVA p-value (Condition pair) < 0.05.

2.14 Statistics

Values reported and shown in graphical displays are the mean +/− standard deviation (S.D.) or standard error of the mean (S.E.M), as indicated. Comparisons of mean expression across groups

were made using an unpaired 2-tailed Student's t test. For all comparisons, p-values less than 0.05 were considered statistically significant.

3 RESULTS

3.1 PIM protein kinase regulates the level of the lncRNA H19

We have chosen to examine two model systems to understand the mechanism by which the family of PIM kinases regulates tumor growth. T-ALL and PCa have been shown to be driven by increased PIM levels, and small molecule inhibitors of PIM decrease the growth of these tumor types. T-ALL cell lines can be divided into the early progenitor type (ETP-ALL), HSB-2, KOPT-K1 and DU.528, containing elevated levels of PIM kinase, and those that are more mature, SUP-T1, HPB-ALL and CUTLL1, and express lower levels of this protein kinase (Padi et al., 2017). ETP-ALL cells are blocked in their growth by PIM inhibitors (PIM-i), while the more mature T-ALLs, SUP-T1 and CUTLL1 are not (Padi et al., 2017). To understand the genes or pathways that might be involved in the sensitivity of HSB-2, KOPT-K1 and DU.528 and the resistance of SUP-T1, HPB-ALL and CUTLL1 to PIM-i, microarray profiling was carried out on these six T-ALL cell lines (Fig. 1A, Table S1). Among the genes most elevated in ETP-ALL cells whose growth is driven by PIM and sensitive to PIM-i therapy, the lncRNA H19 was identified (Fig. 1A). Using qPCR, we confirmed that H19 is highly expressed in the PIM-driven PIM-i sensitive HSB-2 and DU.528 but at much lower levels in the PIM-i insensitive SUP-T1 and CUTLL1 cells (Fig. 1B,C, Fig. S1). Knockdown (KD) of PIM1 levels in HSB-2 with siRNA, led to a significant decrease in cellular H19 level (Fig. 1D), demonstrating that PIM1 regulates H19 in these ETP-ALL cells. Conversely, PIM1 overexpression in the PIM-i resistant cell line SUP-T1 induced increases in H19 levels (Fig. 1E). The PIM1 overexpression in SUP-T1E cells was confirmed by measuring p-IRS1 (S-1101) (Fig. 1E). IRS1 is a known PIM kinase substrate and its phosphorylation is regulated by PIM kinase activity (Song et al., 2016).

A possible mechanism by which PIM regulates H19 levels is by modulation of the H19 DMR methylation. There is a striking difference in the methylation state of H19 between PCa and benign prostate hyperplasia (BPH). 80% of the CpGs in the DMRs and in the ICRs are methylated in BPH, while only 41% of CpGs are methylated in PCa (Paradowska et al., 2009). Bisulfite sequencing demonstrates that while the DMR is methylated in 100% of the SUP-T1 clones, PIM1 overexpressing SUP-T1 cells demonstrated a demethylation of the DMR in 30% of the clones analyzed, reflecting the loss of imprinting of H19 (Fig. S2 A,B). This result suggests a potential mechanism for the suppression of H19 expression in SUP-T1 cells and its potential regulation by PIM1 kinase.

Since PIM1 kinases have been shown to drive the growth of PCa, we sought to address whether the PIM1 regulation of H19 levels was also present in this tumor type. Transient overexpression of PIM1 in human PCa cell lines PC3 and DU145 elevated H19 expression (Fig. 2A, Fig. 2B). To examine whether the kinase activity of this enzyme was needed, DU145 cells were transfected with PIM1 (WT) or a K67M kinase-dead (KiD) mutant (Cen et al., 2010) (Fig. 2B). WT-PIM1, but not its KiD mutant, induced increases in H19 levels (Fig. 2B). Similarly, in human prostate stromal cell line BHPrS1 containing doxycycline (Dox)-inducible PIM1 construct (Zemskova et al., 2015), PIM1 induction resulted in increases in H19 levels which were blocked by 24h of PIM-i (AZD1208, 3μM) treatment (Fig. 2C). The effect of Dox induction and PIM-i treatment were confirmed by p-IRS1 phosphorylation (Fig. 2C). Similarly, PIM1 mediated H19 induction was also observed in normal human prostate derived epithelial cells, hPrEC, (Fig. 2D) or prostate tumor cell line PC3 (Fig. 2E). To check if this H19 induction by PIM kinase is isoform specific, we transduced PC3 cells with PIM1, 2, or 3 and measured the H19 levels. Each of the PIM kinase isoforms induced similar H19 level increases (Fig. S3A), indicating that each isoform was capable of regulating this lncRNA.

H19 and IGF2 are expressed from the same genetic locus (Gabory et al., 2010). We observed no changes in IGF2 RNA expression when PIM1 kinase was transfected in PC3 cells (Fig. 2F). Since H19 has been shown to be directly activated by c-MYC (Barsyte-Lovejoy et al., 2006), the increase in H19 upon PIM overexpression could be mediated by changes in c-MYC levels. It has been shown that the PIM1/PIM2 kinases synergize with c-MYC to induce tumorigenesis. It has been found that overexpressing PIM1 kinase decreased phosphorylation of Thr58 and enhanced phosphorylation at S62 whereas PIM2 caused S329 phosphorylation on c-MYC. These phosphorylation events caused by PIM1/PIM2 lead to increased protein stability and enhanced transcriptional activity of c-MYC.(Kim et al., 2010; Zhang et al., 2008). However, in our model system overexpression of c-MYC in DU145 cells did not induce H19, suggesting that PIM regulates H19 independently of c-MYC function (Fig. S4). Taken together, these data demonstrate that the lncRNA H19 expression is regulated by the PIM kinases in both hematopoietic and solid tumor types.

3.2 PIM overexpression is associated with a stem cell signature

H19 expression has been shown to positively correlate with the level of stem cell genes and pluripotency factors in various tumor types (Bauderlique-Le Roy et al., 2015; Li et al., 2016; Peng et al., 2017; Zeira et al., 2015). Comparison of the PIM-i resistant (SUP-T1, CUTLL1) and sensitive (HSB-2, DU.528) T-ALL cells lines revealed significantly elevated SOX2 expression in

sensitive vs resistant T-ALL cells (Fig. S1). PIM1 overexpression in both T-ALL cell line- SUP-T1 and PCa cell lines- PC3 and DU145, was able to induce the expression of stem cell factors OCT-4, SOX2, NANOG and KLF4 (Fig. 3A,B). At the protein level, PIM1 overexpression in murine PCa cells mPrEC (Song et al., 2018) augmented the level of the stem cell genes Sox2, Nanog and Oct-4 (Fig. 3C). The overexpression of PIM2 and PIM3 in PC3 cells also led to increases in NANOG and OCT-4 gene expression (Fig. S3A). Using a luciferase reporter controlled by either the OCT-4 proximal or distal enhancers, increasing PIM1 levels in PC3 cells showed increased OCT-4 transcription and promoter activity when PIM1 was induced (Fig. 3D). To confirm that the PIM1 induced stem cell signature is associated with a stemness state, we analyzed PIM1 overexpressing cells for the enrichment of stem cell surface markers (CD24 (Weng et al., 2019), CD29 (Lawson et al., 2010; Vassilopoulos et al., 2014), and CD49B (Erb et al., 2018; Lawson et al., 2010)). We demonstrate that PIM1 overexpression in PC3 cells induces stem cell surface markers CD29, CD49b and CD24, suggesting that increased PIM1 expression is capable of inducing a stem cell-like surface phenotype through in part regulating these gene changes (Fig. S3B).

To evaluate the effect of PIM1 overexpression on growth of normal stem cells, we isolated wild type mouse prostate organoids that have been shown to possess stem cell like characteristics (Karthaus et al., 2014). PIM1 overexpression in these organoids caused a significant increase in proliferation of these cells (Fig. 4A; PIM1-RFP vs EV-RFP, $p<0.001$). As in PCa cell lines, overexpressing PIM1 in mouse organoids induced increases in H19 as well as the stem cell genes Klf4, Oct-4, and Sox2 (Fig. 4B). Importantly, in PC3-LN4 cells, a metastatic variant of PC3 cells which expresses elevated levels of the PIM kinases (Song et al., 2018), H19 KD repressed the expression of NANOG, OCT-4, SOX2, and KLF4 (Fig. 4C).

To validate that the PIM1 increases in stem cell genes is mediated by H19, we knocked down H19 in PIM1 overexpressing SUP-T1E cells using either lentivirus encoding scrambled shRNA as a control or shH19 (Fig. 4D). Our results indicated that the knockdown of H19 abrogated the PIM1 induced stem cell gene expression. Thus, these experiments help to establish a novel signaling cascade connecting PIM1, H19, and stem cell genes, suggesting that the PIM1 induction of stem cell genes may occur with the activity of H19.

3.3 PIM-i treatment reduces H19 expression and inhibits cell growth

To investigate the effect of pharmacological inhibition of PIM kinases on the levels of H19 in T-ALL cell lines, HSB-2, DU.528 and CUTLL1 were treated with the pan-PIM-i AZ1208 (3μM, 24h).

This treatment reduced H19 levels in the two ETP-ALL cell lines, HSB-2 and DU.528 by approximately 60%, while it had no effect on H19 levels in the more mature and kinase inhibitor resistant CUTLL1 cells (Fig. 4E). Similarly, treatment of LNCaP cells (Fig. 4F) with PIM-i decreased H19 levels. Similar results were obtained in NEPC cell line LASCPC-01 where PIM447, another small molecule pan-PIM-i, significantly decreased H19, NANOG, OCT-4 and SOX2 expression in a dose-dependent manner (Fig. S5). Additionally, we observed that overexpression of PIM1 partially sensitized PIM-i resistant SUP-T1E cells to PIM-i treatment (Fig. S6). These data demonstrate that PIM1 regulates H19 levels in PIM-dependent but not in PIM-i insensitive cell lines.

To analyze whether the inhibition of PIM and the subsequent decrease in H19 affected cell growth in PCa, we performed XTT assay on PC3 cells with H19 KD and treated or not with a PIM-i. The combination of si-H19 and PIM-i significantly inhibited cell growth (Fig. 5A) while individual treatments had modest effects. NEPC is a variant of PCa that is clinically unresponsive to chemotherapy treatments. To test this combination treatment in this PCa tumor type, we utilized NEPC patient derived organoids OWCM-155 (Puca et al., 2018) which have high levels of H19 (Singh et al., manuscript in preparation). When compared to androgen responsive PCa cell line LNCaP, these organoids have elevated PIM kinase expression (Fig. S7). Stable knockdown of H19 in these organoids (Fig. S8) results in a significant growth reduction (Fig. 5B). When H19 knockdown and PIM-i treatment are combined there is an even further decrease in the NEPC organoid growth (Fig. 5B). These results demonstrate that kinase inhibition and decreases in this lncRNA can function together to inhibit PCa growth.

3.4 H19 blocks the ability of PIM-i to sensitizes prostate cancer cells to hormone blockade

Patients diagnosed with advanced PCa initially respond to androgen deprivation therapy (ADT) but ultimately develop hormone-refractory disease that leads to death. Recent evidence suggests that increased expression of the reprogramming stem cell transcription factor SOX2 makes PCa cells resistant to hormone blockade by the anti-androgen Enza (Mu et al., 2017). To investigate the role of PIM kinases in ADT, we analyzed the effect of Enza treatment on PIM1 overexpressing androgen-responsive PCa cell line LNCaP cells. Interestingly, we observed that while Enza treatment (48h, 10μM) was cytotoxic to the empty vector transduced control LNCaP cells (EV), overexpression of PIM1 caused resistance to Enza treatment (Fig. 5C). This result is consistent with our finding that PIM kinase activity stimulates increases in SOX2 (Fig. 3C). To explore this further, we examined the growth of LNCaP with control vector transduction (LNCaP-EV) and H19 overexpression (LNCaP-H19) (Fig. S9), followed by treatment with increasing concentrations of

PIM447 with or without Enza (2μM, 5μM) treatment for 72h (Fig. 5D,E). The PIM-i treatment significantly sensitized the control LNCaP cells to growth inhibition by Enza (Fig. 5D). Notably, Combosyn analysis (Chou, 2010) demonstrated that the PIM447 and Enza combination was highly synergistic in killing LNCaP cells. As shown in the Fig. S9, the combination index (CI) values were less than 1 for multiple PIM447 and Enza combination doses. Overexpression of H19 in LNCaP cells blocked the effect of PIM kinase inhibitor treatment (Fig. 5E), suggesting that the PIM-mediated control of H19 levels modulates Enza sensitivity in LNCaP cells.

4 DISCUSSION

Our results identify a unique signaling cascade that regulates the transcription of stem cell genes in both T-ALL and PCa. PIM1 kinase induces the expression of lncRNA H19 which in turn stimulates the transcription of the stem cell genes SOX2, NANOG and OCT-4. We found that the expression of H19 is significantly higher in the T-ALL cell lines with high levels of PIM1 kinase and sensitivity to PIM-i (HSB-2, DU.528, and KOPT-K1) as compared to those with low PIM1 levels and insensitivity to these kinase inhibitors (CUTLL1, HPB-ALL, and SUP-T1). Since PIM kinases (Aksoy et al., 2007; Jimenez-Garcia et al., 2017) and H19 (Peng et al., 2017) have been both shown to be involved in the maintenance of stemness in solid tumors as well as haemopoietic malignancies, we decided to investigate if there is a link between the two in the regulation of stem cell genes. We further demonstrated that PIM-i decreased H19 levels in PIM-i sensitive cell lines (HSB-2 and DU.528) but has no effect on H19 levels in the PIM-i insensitive cell line CUTLL1. Overexpression of PIM1 in SUP-T1 cells increased stem cell gene transcription through H19 and restored partial sensitivity to PIM-i. Further we identified that the stem cell genes SOX2, KLF4, NANOG and OCT-4 were induced as a result of H19 elevation. These findings were corroborated in PCa cells indicating that the PIM regulation of H19 and induction of stem cell genes in both solid and hematopoietic tumors.

Further analysis of the microarray data comparing the transcriptomes of PIM-i sensitive versus insensitive cells revealed enrichment of several pathways important for stem cell progression and maintenance (Table S2) in the PIM-i sensitive cell lines. Studies have shown the involvement of these pathways in maintenance of pluripotent stem cells both in solid tumors as well as hematopoietic malignancies. (Madsen et al., 2019; O'Donnell et al., 2016). Further experiments are needed to examine the role of PIM and H19 in regulating a broad segment of the genes regulating this stem cell phenotype.

The mechanism by which H19 mediates stemness in liquid and solid tumors (Jiang et al., 2016; Peng et al., 2017; Ren et al., 2018; Sasaki et al., 2018) (Zhou et al., 2019) is likely complex. Various studies have pointed out the “sponge effect” of H19 in which this lncRNA decreases the bioavailability of miRNAs such as Let7 leading to an increase their target gene expression (RAS, MYC, HMGA2, STAT3, IL10) (Peng et al., 2017; Zhou et al., 2017). H19 forms a double-negative circuit with let-7 and LIN28 in breast cancer cells, wherein H19 sponges the let7 miRNA that consequently releases and promotes the LIN28 expression. This increase in LIN28 expression further potentiates H19 expression leading to the feedback circuit that acts to maintain the stem cell state in breast cancer (Peng et al., 2017). The LIN28/let7 have also been associated with

increasing the stem cell gene expression in oral squamous cell carcinoma (Chien et al., 2015). The suppression of Let7 by LIN28 de-represses its target mRNAs- ARID3B and HMGA2, which then is thought to increase the transcription of stem cell genes OCT-4 and SOX2, through promoter binding. However, further studies are needed to investigate the effect of H19 on this double negative feedback loop in the context of PIM1 overexpressing PCa or T-ALL cells.

Alternatively, H19 may function to increase stem cell gene levels through epigenetic mechanisms. H19 has been documented to bind to S-adenosylhomocysteine hydrolase protein inducing genome wide methylation changes by indirectly regulating S-adenosylmethionine dependent methyl transferases (Zhou et al., 2015). This H19 driven methylation could be sufficient to increase the transcription of stem cell genes. It has been demonstrated by our laboratory (Singh et al., manuscript in preparation) and others that H19 physically interacts with the proteins in the PRC2 complex e.g. EZH2, and increases histone H3K27me3 modifications (Fazi et al., 2018). It is possible that similar to the lncRNA HOTAIR (Tsai et al., 2010), H19 could bind both the PRC2 complex and lysine demethylases to mutually activate and repress gene transcription inducing a "stem-like" state.

The PIM kinases may function to elevate H19 levels by regulating both transcription factor binding and DNA methylation. The promoter region of H19 contains transcription factor binding sites for HIF1 (Wu et al., 2017), AR (putative), E2F1 (Berteaux et al., 2005) and OCT-4/SOX2 (Zimmerman et al., 2013). In hypoxia, PIM kinases are elevated and increase HIF1 activity (Casillas et al., 2018), thus having the potential to activate H19 transcription. H19 levels have been shown to be hormonally regulated and are inhibited by dihydrotestosterone in androgen responsive cells (Berteaux et al., 2004), thus pointing to an inverse relation between AR and H19. PIM1 can regulate AR levels by phosphorylation leading to degradation of this protein (Linn et al., 2012) potentially removing a negative regulator controlling the transcription of this lncRNA.

All the PIM isoforms phosphorylate p27 protein leading to its degradation, stimulating the cell cycle (Morishita et al., 2008) which can indirectly inhibit RB activity. When RB1 activity is lost, E2F1 could bind to the H19 promoter and stimulate increases in its transcription (Berteaux et al., 2005). In turn, H19 affects RB1 phosphorylation by regulating the expression of CDK4 and CCND1 genes (Ohtsuka et al., 2016) that can act to further increase E2F1 activity. In murine embryonic stem cells OCT-4 and SOX2 have been shown to cooperatively bind the ICR of the Igf2/H19 locus, resulting in a hypomethylated state which stimulates increases in this lncRNA (Zimmerman et al., 2013). Mass spectrometry on PIM1 treated ES cell samples revealed the relative abundance of phosphorylated OCT4 peptides that contain putative PIM1 phosphorylation

at S289 and S290 suggesting that PIM1 phosphorylates OCT-4 (Brumbaugh et al., 2012). PIM kinase inhibitor treatment could block this phosphorylation inhibiting the ability of OCT-4 to work synergistically with SOX2. Consequently, the decreased binding of these two transcription factors could reduce H19 levels.

We showed that expression of PIM1 in T-ALL modulates the methylation status of H19 DMR suggesting that the PIM kinase could act directly or indirectly as an epigenetic regulator. It has been suggested that PIM regulates DNA methylation. Phosphorylation of heterochromatin protein 1γ (HP1) at Ser-93 by PIM1 promotes HP1 binding with histone H3K9me3, which leads to heterochromatin formation and the suppression of gene transcription responsible for proliferation (Jin et al., 2014). Further experiments are required to decipher the exact mechanism by which PIM controls H19 levels.

PCa cells can escape androgen deprivation therapy through a change in lineage identity driven by elevated SOX2. Knocking down SOX2 can restore sensitivity to Enza *in vitro* and in mouse xenograft models (Mu et al., 2017). Our findings are consistent with these observations in that small molecule PIM-i downregulate SOX2 and sensitize androgen-responsive LNCaP cells to Enza therapy. This result could be secondary to the ability of these inhibitors to decrease H19. Alternatively, the long form of PIM1 phosphorylates AR on Thr-850 thereby stabilizing AR by recruiting the ubiquitin E3 ligase RNF6 (Linn et al., 2012). This stabilization could promote AR-mediated transcription under low-androgen conditions. A recent study (Lawrence et al., 2018) showed that the combination of pan-PIM-i with RNA polymerase I inhibitor targeting ribosomal biosynthesis was effective against all four neuroendocrine-like AR-null patient-derived xenografts. These tumor cells exhibited heterogeneous mechanisms of resistance, including AR mutations and genomic structural rearrangements of the AR gene (Lawrence et al., 2018).

5 CONCLUSIONS

Our data demonstrates that PIM kinase induction increases the lncRNA H19 and this in turn regulates stem cell genes, including the transcription factor SOX2 which plays a role in controlling the response to ADT. Additionally, we found that while elevated levels of PIM1 contributes resistance to ADT, the combination of a pan-PIM inhibitor and H19 knockdown can reduce the tumor forming capacity of highly aggressive NEPC. Together these data suggest a novel pathway controlled by the PIM kinases whose inhibition could impact clinical outcomes.

Author Contributions

N.S., V.O. and A.S.K. wrote the manuscript.

N.S., S.K.R.P., J.J.B., R.P., J.H.S., and V.O. designed and carried out the experiments.

K.O. and H.B. supplied essential reagents.

N.S., V.O. and A.S.K. conceived the project.

Funding

This study was supported by University of Arizona Cancer Center (UACC) grant P30CA023074, Department of Defense award W81XWH-18-1-0533 (N.S.), National Institute of Health award R01CA173200 (A.S.K.) and Department of Defense award W81XWH-12-1-0560 (A.S.K.).

Acknowledgments

The authors wish to thank Novartis Pharmaceuticals for providing PIM447. The UACC Shared Resources carried out flow cytometric analysis. We wish to thank Dr. Marina Cardó Vila for her helpful suggestions and review of this manuscript.

Disclosure of potential conflicts of interest

The authors declare no potential conflicts of interest.

References

Adriaenssens, E., Dumont, L., Lottin, S., Bolle, D., Lepretre, A., Delobelle, A., Bouali, F., Dugimont, T., Coll, J., Curgy, J.J., 1998. H19 overexpression in breast adenocarcinoma stromal cells is associated with tumor values and steroid receptor status but independent of p53 and Ki-67 expression. Am J Pathol 153, 1597-1607.

Aksoy, I., Sakabedoyan, C., Bourillot, P.Y., Malashicheva, A.B., Mancip, J., Knoblauch, K., Afanassieff, M., Savatier, P., 2007. Self-renewal of murine embryonic stem cells is supported by the serine/threonine kinases Pim-1 and Pim-3. Stem Cells 25, 2996-3004.

Alizadeh, A.A., Eisen, M.B., Davis, R.E., Ma, C., Lossos, I.S., Rosenwald, A., Boldrick, J.C., Sabet, H., Tran, T., Yu, X., Powell, J.I., Yang, L., Marti, G.E., Moore, T., Hudson, J., Jr., Lu, L., Lewis, D.B., Tibshirani, R., Sherlock, G., Chan, W.C., Greiner, T.C., Weisenburger, D.D., Armitage, J.O., Warnke, R., Levy, R., Wilson, W., Grever, M.R., Byrd, J.C., Botstein, D., Brown, P.O., Staudt, L.M., 2000. Distinct types of diffuse large B-cell lymphoma identified by gene expression profiling. Nature 403, 503-511.

An, N., Lin, Y.W., Mahajan, S., Kellner, J.N., Wang, Y., Li, Z., Kraft, A.S., Kang, Y., 2013. Pim1 serine/threonine kinase regulates the number and functions of murine hematopoietic stem cells. Stem Cells 31, 1202-1212.

Ariel, I., Lustig, O., Schneider, T., Pizov, G., Sappir, M., De-Groot, N., Hochberg, A., 1995. The imprinted H19 gene as a tumor marker in bladder carcinoma. Urology 45, 335-338.

Barsyte-Lovejoy, D., Lau, S.K., Boutros, P.C., Khosravi, F., Jurisica, I., Andrulis, I.L., Tsao, M.S., Penn, L.Z., 2006. The c-Myc oncogene directly induces the H19 noncoding RNA by allele-specific binding to potentiate tumorigenesis. Cancer Res 66, 5330-5337.

Bauderlique-Le Roy, H., Vennin, C., Brocqueville, G., Spruyt, N., Adriaenssens, E., Bourette, R.P., 2015. Enrichment of Human Stem-Like Prostate Cells with s-SHIP Promoter Activity Uncovers a Role in Stemness for the Long Noncoding RNA H19. Stem Cells Dev 24, 1252-1262.

Ben-Porath, I., Thomson, M.W., Carey, V.J., Ge, R., Bell, G.W., Regev, A., Weinberg, R.A., 2008. An embryonic stem cell-like gene expression signature in poorly differentiated aggressive human tumors. Nat Genet 40, 499-507.

Berteaux, N., Lottin, S., Adriaenssens, E., Van Coppenolle, F., Leroy, X., Coll, J., Dugimont, T., Curgy, J.J., 2004. Hormonal regulation of H19 gene expression in prostate epithelial cells. J Endocrinol 183, 69-78.

Berteaux, N., Lottin, S., Monte, D., Pinte, S., Quatannens, B., Coll, J., Hondermarck, H., Curgy, J.J., Dugimont, T., Adriaenssens, E., 2005. H19 mRNA-like noncoding RNA promotes breast cancer cell proliferation through positive control by E2F1. J Biol Chem 280, 29625-29636.

Brady, J.J., Li, M., Suthram, S., Jiang, H., Wong, W.H., Blau, H.M., 2013. Early role for IL-6 signalling during generation of induced pluripotent stem cells revealed by heterokaryon RNA-Seq. Nat Cell Biol 15, 1244-1252.

Brault, L., Gasser, C., Bracher, F., Huber, K., Knapp, S., Schwaller, J., 2010. PIM serine/threonine kinases in the pathogenesis and therapy of hematologic malignancies and solid cancers. Haematologica 95, 1004-1015.

Brumbaugh, J., Hou, Z., Russell, J.D., Howden, S.E., Yu, P., Ledvina, A.R., Coon, J.J., Thomson, J.A., 2012. Phosphorylation regulates human OCT4. Proc Natl Acad Sci U S A 109, 7162-7168.

Casillas, A.L., Toth, R.K., Sainz, A.G., Singh, N., Desai, A.A., Kraft, A.S., Warfel, N.A., 2018. Hypoxia-Inducible PIM Kinase Expression Promotes Resistance to Antiangiogenic Agents. Clin Cancer Res 24, 169-180.

Cen, B., Mahajan, S., Zemskova, M., Beharry, Z., Lin, Y.W., Cramer, S.D., Lilly, M.B., Kraft, A.S., 2010. Regulation of Skp2 levels by the Pim-1 protein kinase. J Biol Chem 285, 29128-29137.

Chen, W.W., Chan, D.C., Donald, C., Lilly, M.B., Kraft, A.S., 2005. Pim family kinases enhance tumor growth of prostate cancer cells. Mol Cancer Res 3, 443-451.

Chien, C.S., Wang, M.L., Chu, P.Y., Chang, Y.L., Liu, W.H., Yu, C.C., Lan, Y.T., Huang, P.I., Lee, Y.Y., Chen, Y.W., Lo, W.L., Chiou, S.H., 2015. Lin28B/Let-7 Regulates Expression of Oct4 and Sox2 and Reprograms Oral Squamous Cell Carcinoma Cells to a Stem-like State. Cancer Res 75, 2553-2565.

Chou, T.C., 2010. Drug combination studies and their synergy quantification using the Chou-Talalay method. Cancer Res 70, 440-446.

Cibull, T.L., Jones, T.D., Li, L., Eble, J.N., Ann Baldridge, L., Malott, S.R., Luo, Y., Cheng, L., 2006. Overexpression of Pim-1 during progression of prostatic adenocarcinoma. J Clin Pathol 59, 285-288.

Cohen, A.M., Grinblat, B., Bessler, H., Kristt, D., Kremer, A., Schwartz, A., Halperin, M., Shalom, S., Merkel, D., Don, J., 2004. Increased expression of the hPim-2 gene in human chronic lymphocytic leukemia and non-Hodgkin lymphoma. Leuk Lymphoma 45, 951-955.

Cuypers, H.T., Selten, G., Quint, W., Zijlstra, M., Maandag, E.R., Boelens, W., van Wezenbeek, P., Melief, C., Berns, A., 1984. Murine leukemia virus-induced T-cell lymphomagenesis: integration of proviruses in a distinct chromosomal region. Cell 37, 141-150.

Davies, A.H., Beltran, H., Zoubeidi, A., 2018. Cellular plasticity and the neuroendocrine phenotype in prostate cancer. Nat Rev Urol 15, 271-286.

Drost, J., Karthaus, W.R., Gao, D., Driehuis, E., Sawyers, C.L., Chen, Y., Clevers, H., 2016. Organoid culture systems for prostate epithelial and cancer tissue. Nat Protoc 11, 347-358.

Elkin, M., Shevelev, A., Schulze, E., Tykocinsky, M., Cooper, M., Ariel, I., Pode, D., Kopf, E., de Groot, N., Hochberg, A., 1995. The expression of the imprinted H19 and IGF-2 genes in human bladder carcinoma. FEBS Lett 374, 57-61.

Erb, H.H.H., Guggenberger, F., Santer, F.R., Culig, Z., 2018. Interleukin-4 induces a CD44high /CD49bhigh PC3 subpopulation with tumor-initiating characteristics. J Cell Biochem 119, 4103-4112.

Fazi, B., Garbo, S., Toschi, N., Mangiola, A., Lombari, M., Sicari, D., Battistelli, C., Galardi, S., Michienzi, A., Trevisi, G., Harari-Steinfeld, R., Cicchini, C., Ciafre, S.A., 2018. The lncRNA H19 positively affects the tumorigenic properties of glioblastoma cells and contributes to NKD1 repression through the recruitment of EZH2 on its promoter. Oncotarget 9, 15512-15525.

Gabory, A., Jammes, H., Dandolo, L., 2010. The H19 locus: role of an imprinted non-coding RNA in growth and development. Bioessays 32, 473-480.

Gafni, O., Weinberger, L., Mansour, A.A., Manor, Y.S., Chomsky, E., Ben-Yosef, D., Kalma, Y., Viukov, S., Maza, I., Zviran, A., Rais, Y., Shipony, Z., Mukamel, Z., Krupalnik, V., Zerbib, M., Geula, S., Caspi, I., Schneir, D., Shwartz, T., Gilad, S., Amann-Zalcenstein, D., Benjamin, S., Amit, I., Tanay, A., Massarwa, R., Novershtern, N., Hanna, J.H., 2013. Derivation of novel human ground state naive pluripotent stem cells. Nature 504, 282-286.

Gu, G., Yuan, J., Wills, M., Kasper, S., 2007. Prostate cancer cells with stem cell characteristics reconstitute the original human tumor in vivo. Cancer Res 67, 4807-4815.

Hibi, K., Nakamura, H., Hirai, A., Fujikake, Y., Kasai, Y., Akiyama, S., Ito, K., Takagi, H., 1996. Loss of H19 imprinting in esophageal cancer. Cancer Res 56, 480-482.

Jiang, X., Yan, Y., Hu, M., Chen, X., Wang, Y., Dai, Y., Wu, D., Wang, Y., Zhuang, Z., Xia, H., 2016. Increased level of H19 long noncoding RNA promotes invasion, angiogenesis, and stemness of glioblastoma cells. J Neurosurg 124, 129-136.

Jimenez-Garcia, M.P., Lucena-Cacace, A., Robles-Frias, M.J., Ferrer, I., Narlik-Grassow, M., Blanco-Aparicio, C., Carnero, A., 2017. Inflammation and stem markers association to PIM1/PIM2 kinase-induced tumors in breast and uterus. Oncotarget 8, 58872-58886.

Jin, B., Wang, Y., Wu, C.L., Liu, K.Y., Chen, H., Mao, Z.B., 2014. PIM-1 modulates cellular senescence and links IL-6 signaling to heterochromatin formation. Aging Cell 13, 879-889.

Karthaus, W.R., Iaquinta, P.J., Drost, J., Gracanin, A., van Boxtel, R., Wongvipat, J., Dowling, C.M., Gao, D., Begthel, H., Sachs, N., Vries, R.G.J., Cuppen, E., Chen, Y., Sawyers, C.L., Clevers, H.C., 2014. Identification of multipotent luminal progenitor cells in human prostate organoid cultures. Cell 159, 163-175.

Kim, J., Roh, M., Abdulkadir, S.A., 2010. Pim1 promotes human prostate cancer cell tumorigenicity and c-MYC transcriptional activity. BMC Cancer 10, 248.

Kondo, M., Suzuki, H., Ueda, R., Osada, H., Takagi, K., Takahashi, T., Takahashi, T., 1995. Frequent loss of imprinting of the H19 gene is often associated with its overexpression in human lung cancers. Oncogene 10, 1193-1198.

Lawrence, M.G., Obinata, D., Sandhu, S., Selth, L.A., Wong, S.Q., Porter, L.H., Lister, N., Pook, D., Pezaro, C.J., Goode, D.L., Rebello, R.J., Clark, A.K., Papargiris, M., Van Gramberg, J., Hanson, A.R., Banks, P., Wang, H., Niranjan, B., Keerthikumar, S., Hedwards, S., Huglo, A., Yang, R., Henzler, C., Li, Y., Lopez-Campos, F., Castro, E., Toivanen, R., Azad, A., Bolton, D., Goad, J., Grummet, J., Harewood, L., Kourambas, J., Lawrentschuk, N., Moon, D., Murphy, D.G., Sengupta, S., Snow, R., Thorne, H., Mitchell, C., Pedersen, J., Clouston, D., Norden, S., Ryan, A., Dehm, S.M., Tilley, W.D., Pearson, R.B., Hannan, R.D., Frydenberg, M., Furic, L., Taylor, R.A., Risbridger, G.P., 2018. Patient-derived Models of Abiraterone- and Enzalutamide-resistant Prostate Cancer Reveal Sensitivity to Ribosome-directed Therapy. Eur Urol 74, 562-572.

Lawson, D.A., Zong, Y., Memarzadeh, S., Xin, L., Huang, J., Witte, O.N., 2010. Basal epithelial stem cells are efficient targets for prostate cancer initiation. Proc Natl Acad Sci U S A 107, 2610-2615.

Lee, C., Kim, S.J., Na, J.Y., Park, C.S., Lee, S.Y., Kim, I.H., Oh, Y.K., 2003. Alterations in Promoter Usage and Expression Levels of Insulin-like Growth Factor-II and H19 Genes in Cervical and Endometrial Cancer. Cancer Res Treat 35, 314-322.

Li, W., Jiang, P., Sun, X., Xu, S., Ma, X., Zhan, R., 2016. Suppressing H19 Modulates Tumorigenicity and Stemness in U251 and U87MG Glioma Cells. Cell Mol Neurobiol 36, 1219-1227.

Linn, D.E., Yang, X., Xie, Y., Alfano, A., Deshmukh, D., Wang, X., Shimelis, H., Chen, H., Li, W., Xu, K., Chen, M., Qiu, Y., 2012. Differential regulation of androgen receptor by PIM-1 kinases via phosphorylation-dependent recruitment of distinct ubiquitin E3 ligases. J Biol Chem 287, 22959-22968.

Madsen, R.R., Knox, R.G., Pearce, W., Lopez, S., Mahler-Araujo, B., McGranahan, N., Vanhaesebroeck, B., Semple, R.K., 2019. Oncogenic PIK3CA promotes cellular stemness in an allele dose-dependent manner. Proc Natl Acad Sci U S A 116, 8380-8389.

Markert, E.K., Mizuno, H., Vazquez, A., Levine, A.J., 2011. Molecular classification of prostate cancer using curated expression signatures. Proc Natl Acad Sci U S A 108, 21276-21281.

Mathieu, J., Zhang, Z., Zhou, W., Wang, A.J., Heddleston, J.M., Pinna, C.M., Hubaud, A., Stadler, B., Choi, M., Bar, M., Tewari, M., Liu, A., Vessella, R., Rostomily, R., Born, D., Horwitz, M., Ware, C., Blau, C.A., Cleary, M.A., Rich, J.N., Ruohola-Baker, H., 2011. HIF induces human embryonic stem cell markers in cancer cells. Cancer Res 71, 4640-4652.

Morishita, D., Katayama, R., Sekimizu, K., Tsuruo, T., Fujita, N., 2008. Pim kinases promote cell cycle progression by phosphorylating and down-regulating p27Kip1 at the transcriptional and posttranscriptional levels. Cancer Res 68, 5076-5085.

Mu, P., Zhang, Z., Benelli, M., Karthaus, W.R., Hoover, E., Chen, C.C., Wongvipat, J., Ku, S.Y., Gao, D., Cao, Z., Shah, N., Adams, E.J., Abida, W., Watson, P.A., Prandi, D., Huang, C.H., de Stanchina, E., Lowe, S.W., Ellis, L., Beltran, H., Rubin, M.A., Goodrich, D.W., Demichelis, F., Sawyers, C.L., 2017. SOX2 promotes lineage plasticity and antiandrogen resistance in TP53- and RB1-deficient prostate cancer. Science 355, 84-88.

Ngo, V.N., Davis, R.E., Lamy, L., Yu, X., Zhao, H., Lenz, G., Lam, L.T., Dave, S., Yang, L., Powell, J., Staudt, L.M., 2006. A loss-of-function RNA interference screen for molecular targets in cancer. Nature 441, 106-110.

O'Donnell, R.K., Falcon, B., Hanson, J., Goldstein, W.E., Perruzzi, C., Rafii, S., Aird, W.C., Benjamin, L.E., 2016. VEGF-A/VEGFR Inhibition Restores Hematopoietic Homeostasis in the Bone Marrow and Attenuates Tumor Growth. Cancer Res 76, 517-524.

Ohtsuka, M., Ling, H., Ivan, C., Pichler, M., Matsushita, D., Goblirsch, M., Stiegelbauer, V., Shigeyasu, K., Zhang, X., Chen, M., Vidhu, F., Bartholomeusz, G.A., Toiyama, Y., Kusunoki, M., Doki, Y., Mori, M., Song, S., Gunther, J.R., Krishnan, S., Slaby, O., Goel, A., Ajani, J.A., Radovich, M., Calin, G.A., 2016. H19 Noncoding RNA, an Independent Prognostic Factor, Regulates Essential Rb-E2F and CDK8-beta-Catenin Signaling in Colorectal Cancer. EBioMedicine 13, 113-124.

Pachnis, V., Brannan, C.I., Tilghman, S.M., 1988. The structure and expression of a novel gene activated in early mouse embryogenesis. EMBO J 7, 673-681.

Padi, S.K.R., Luevano, L.A., An, N., Pandey, R., Singh, N., Song, J.H., Aster, J.C., Yu, X.Z., Mehrotra, S., Kraft, A.S., 2017. Targeting the PIM protein kinases for the treatment of a T-cell acute lymphoblastic leukemia subset. Oncotarget 8, 30199-30216.

Paradowska, A., Fenic, I., Konrad, L., Sturm, K., Wagenlehner, F., Weidner, W., Steger, K., 2009. Aberrant epigenetic modifications in the CTCF binding domain of the IGF2/H19 gene in prostate cancer compared with benign prostate hyperplasia. Int J Oncol 35, 87-96.

Peng, F., Li, T.T., Wang, K.L., Xiao, G.Q., Wang, J.H., Zhao, H.D., Kang, Z.J., Fan, W.J., Zhu, L.L., Li, M., Cui, B., Zheng, F.M., Wang, H.J., Lam, E.W., Wang, B., Xu, J., Liu, Q., 2017. H19/let-7/LIN28 reciprocal negative regulatory circuit promotes breast cancer stem cell maintenance. Cell Death Dis 8, e2569.

Peters, T.L., Li, L., Tula-Sanchez, A.A., Pongtornpipat, P., Schatz, J.H., 2016. Control of translational activation by PIM kinase in activated B-cell diffuse large B-cell lymphoma confers sensitivity to inhibition by PIM447. Oncotarget 7, 63362-63373.

Phillips, J.E., Corces, V.G., 2009. CTCF: master weaver of the genome. Cell 137, 1194-1211.

Poirier, F., Chan, C.T., Timmons, P.M., Robertson, E.J., Evans, M.J., Rigby, P.W., 1991. The murine H19 gene is activated during embryonic stem cell differentiation in vitro and at the time of implantation in the developing embryo. Development 113, 1105-1114.

Puca, L., Bareja, R., Prandi, D., Shaw, R., Benelli, M., Karthaus, W.R., Hess, J., Sigouros, M., Donoghue, A., Kossai, M., Gao, D., Cyrta, J., Sailer, V., Vosoughi, A., Pauli, C., Churakova, Y., Cheung, C., Deonarine, L.D., McNary, T.J., Rosati, R., Tagawa, S.T., Nanus, D.M., Mosquera, J.M., Sawyers, C.L., Chen, Y., Inghirami, G., Rao, R.A., Grandori, C., Elemento, O., Sboner, A., Demichelis, F., Rubin, M.A., Beltran, H., 2018. Patient derived organoids to model rare prostate cancer phenotypes. Nat Commun 9, 2404.

Ramnarine, V.R., Alshalalfa, M., Mo, F., Nabavi, N., Erho, N., Takhar, M., Shukin, R., Brahmbhatt, S., Gawronski, A., Kobelev, M., Nouri, M., Lin, D., Tsai, H., Lotan, T.L., Karnes, R.J., Rubin, M.A., Zoubeidi, A., Gleave, M.E., Sahinalp, C., Wyatt, A.W., Volik, S.V., Beltran, H., Davicioni, E., Wang, Y., Collins, C.C., 2018. The long noncoding RNA landscape of neuroendocrine prostate cancer and its clinical implications. Gigascience 7.

Ren, J., Ding, L., Zhang, D., Shi, G., Xu, Q., Shen, S., Wang, Y., Wang, T., Hou, Y., 2018. Carcinoma-associated fibroblasts promote the stemness and chemoresistance of colorectal cancer by transferring exosomal lncRNA H19. Theranostics 8, 3932-3948.

Rybak, A.P., He, L., Kapoor, A., Cutz, J.C., Tang, D., 2011. Characterization of sphere-propagating cells with stem-like properties from DU145 prostate cancer cells. Biochim Biophys Acta 1813, 683-694.

Sasaki, N., Toyoda, M., Yoshimura, H., Matsuda, Y., Arai, T., Takubo, K., Aida, J., Ishiwata, T., 2018. H19 long non-coding RNA contributes to sphere formation and invasion through regulation of CD24 and integrin expression in pancreatic cancer cells. Oncotarget 9, 34719-34734.

Shah, N., Pang, B., Yeoh, K.G., Thorn, S., Chen, C.S., Lilly, M.B., Salto-Tellez, M., 2008. Potential roles for the PIM1 kinase in human cancer - a molecular and therapeutic appraisal. Eur J Cancer 44, 2144-2151.

Song, J.H., Padi, S.K., Luevano, L.A., Minden, M.D., DeAngelo, D.J., Hardiman, G., Ball, L.E., Warfel, N.A., Kraft, A.S., 2016. Insulin receptor substrate 1 is a substrate of the Pim protein kinases. Oncotarget 7, 20152-20165.

Song, J.H., Singh, N., Luevano, L.A., Padi, S.K.R., Okumura, K., Olive, V., Black, S.M., Warfel, N.A., Goodrich, D.W., Kraft, A.S., 2018. Mechanisms Behind Resistance to PI3K Inhibitor Treatment Induced by the PIM Kinase. Mol Cancer Ther 17, 2710-2721.

Takeuchi, S., Hofmann, W.K., Tsukasaki, K., Takeuchi, N., Ikezoe, T., Matsushita, M., Uehara, Y., Phillip Koeffler, H., 2007. Loss of H19 imprinting in adult T-cell leukaemia/lymphoma. Br J Haematol 137, 380-381.

Tiscornia, G., Singer, O., Verma, I.M., 2006. Production and purification of lentiviral vectors. Nature Protocols 1, 241-245.

Tsai, M.C., Manor, O., Wan, Y., Mosammaparast, N., Wang, J.K., Lan, F., Shi, Y., Segal, E., Chang, H.Y., 2010. Long noncoding RNA as modular scaffold of histone modification complexes. Science 329, 689-693.

Vassilopoulos, A., Chisholm, C., Lahusen, T., Zheng, H., Deng, C.X., 2014. A critical role of CD29 and CD49f in mediating metastasis for cancer-initiating cells isolated from a Brca1-associated mouse model of breast cancer. Oncogene 33, 5477-5482.

Weng, C.C., Ding, P.Y., Liu, Y.H., Hawse, J.R., Subramaniam, M., Wu, C.C., Lin, Y.C., Chen, C.Y., Hung, W.C., Cheng, K.H., 2019. Mutant Kras-induced upregulation of CD24 enhances prostate cancer stemness and bone metastasis. Oncogene 38, 2005-2019.

Wingett, D., Long, A., Kelleher, D., Magnuson, N.S., 1996. pim-1 proto-oncogene expression in anti-CD3-mediated T cell activation is associated with protein kinase C activation and is independent of Raf-1. J Immunol 156, 549-557.

Wu, W., Hu, Q., Nie, E., Yu, T., Wu, Y., Zhi, T., Jiang, K., Shen, F., Wang, Y., Zhang, J., You, Y., 2017. Hypoxia induces H19 expression through direct and indirect Hif-1alpha activity, promoting oncogenic effects in glioblastoma. Sci Rep 7, 45029.

Zeira, E., Abramovitch, R., Meir, K., Even Ram, S., Gil, Y., Bulvik, B., Bromberg, Z., Levkovitch, O., Nahmansson, N., Adar, R., Reubinoff, B., Galun, E., Gropp, M., 2015. The knockdown of H19lncRNA reveals its regulatory role in pluripotency and tumorigenesis of human embryonic carcinoma cells. Oncotarget 6, 34691-34703.

Zemel, S., Bartolomei, M.S., Tilghman, S.M., 1992. Physical linkage of two mammalian imprinted genes, H19 and insulin-like growth factor 2. Nat Genet 2, 61-65.

Zemskova, M.Y., Song, J.H., Cen, B., Cerda-Infante, J., Montecinos, V.P., Kraft, A.S., 2015. Regulation of prostate stromal fibroblasts by the PIM1 protein kinase. Cell Signal 27, 135-146.

Zhang, Y., Wang, Z., Li, X., Magnuson, N.S., 2008. Pim kinase-dependent inhibition of c-Myc degradation. Oncogene 27, 4809-4819.

Zhou, J., Xu, J., Zhang, L., Liu, S., Ma, Y., Wen, X., Hao, J., Li, Z., Ni, Y., Li, X., Zhou, F., Li, Q., Wang, F., Wang, X., Si, Y., Zhang, P., Liu, C., Bartolomei, M., Tang, F., Liu, B., Yu, J., Lan, Y., 2019. Combined Single-Cell Profiling of lncRNAs and Functional Screening Reveals that H19 Is Pivotal for Embryonic Hematopoietic Stem Cell Development. Cell Stem Cell 24, 285-298 e285.

Zhou, J., Yang, L., Zhong, T., Mueller, M., Men, Y., Zhang, N., Xie, J., Giang, K., Chung, H., Sun, X., Lu, L., Carmichael, G.G., Taylor, H.S., Huang, Y., 2015. H19 lncRNA alters DNA methylation genome wide by regulating S-adenosylhomocysteine hydrolase. Nat Commun 6, 10221.

Zhou, W., Ye, X.L., Xu, J., Cao, M.G., Fang, Z.Y., Li, L.Y., Guan, G.H., Liu, Q., Qian, Y.H., Xie, D., 2017. The lncRNA H19 mediates breast cancer cell plasticity during EMT and MET plasticity by differentially sponging miR-200b/c and let-7b. Sci Signal 10.

Zimmerman, D.L., Boddy, C.S., Schoenherr, C.S., 2013. Oct4/Sox2 binding sites contribute to maintaining hypomethylation of the maternal igf2/h19 imprinting control region. PLoS One 8, e81962.

Figure Legends

Figure 1. PIM induces H19 expression in T-ALL cell lines. A, Scatter-plot of genes that are significantly different (Fold Change (linear) < − 2 or > + 2 and ANOVA p-value (Condition pair) < 0.05.) comparing the RNA levels of PIM-i sensitive cells to PIM-i resistant T-ALL cell lines. H19 and PIM1 RNA are circled. Expression levels are visualized as color-coded with red indicating higher levels and green lower levels of gene expression. **B**, Relative PIM1 RNA expression in HSB-2, DU.528, SUP-T1 and CUTLL1. **C**, Relative RNA expression of H19 in HSB-2, DU.528, SUP-T1 and CUTLL1. **D**, Relative RNA expression of H19 and PIM1 in HSB-2 cells transfected with an siRNA to a negative control (siNC as control) or PIM1 (si-PIM1). **E**, Relative RNA expression of PIM1 and H19 in SUP-T1 cells that were engineered (SUP-T1E) for infection with control vector MigR1 (SUP-T1E MigR1) or PIM1 overexpressing vector MigPIM1 (SUP-T1E MigPIM1). The Western blot (WB) was performed with the indicated antibodies. ACTIN was used as loading control. **B-E**, Relative RNA expression were normalized to 18S RNA levels. Values are mean +/- SEM; n=3; *p<0.05, **p<0.01, ***p<0.001.

Figure 2. PIM1 induces H19 expression in prostate cancer cell lines. A, Relative H19 RNA expression in PC3 cells transfected with empty vector (EV) as control or FUCRW-PIM1 (PIM1). PIM1 protein expression was validated by WB. **B,** Relative H19 RNA expression in DU145 cells transfected with pcDNA3 vector encoding either PIM1 (PIM1) or a mutated kinase-dead PIM1 (PIM1-KiD). DU145 (EV) cells were used as control. Respective transfections and PIM1 overexpression were validated by WB. **C,** Relative H19 RNA expression in BHPrS1 cells stably expressing Tripz vector encoding Dox-inducible PIM1 (BHPrS1 Tripz-PIM1). H19 expression level was measured by qPCR after Dox treatment (20ng/ml, 24h) with or without overnight incubation with PIM-i (3μM, AZD1208). The WB was performed with the indicated antibodies. **D**, Relative H19 RNA expression in normal human prostate derived epithelial cells, hPrEC cells stably expressing Tripz vector encoding Dox-inducible PIM1. H19 expression level was measured after Dox treatment (20ng/ml, 24h) by qPCR. **E**, Relative H19 RNA expression in PC3 cells stably expressing Tripz vector encoding Dox-inducible PIM1 (PC3 Tripz-PIM1). H19 expression level was measured after Dox treatment (20ng/ml, 24h) by qPCR. Western blot (WB) was performed with the indicated antibodies. Inhibitor treatments are the same as in C. **F,** Relative H19 and IGF2 RNA expression in PC3 cells transfected with empty vector (EV) as control or FUCRW-PIM1 (PIM1). **A-C, E,** For WB: ACTIN was used as loading control. Numerical values shown under the blot are derived as described in Materials, and calculated relative to the Controls. **A-F,** Relative

RNA expression was normalized to 18S RNA levels. Values are mean +/- SEM; n=3; n.s.= not significant, *p<0.05, **p<0.01, ***p<0.001.

Figure 3. PIM1 regulates stem cells genes in T-ALL and prostate cancer cell lines. A, Relative RNA expression of H19, KLF4, NANOG, OCT-4 and SOX2 in SUP-T1E cells transfected with control MigR1 vector (MigR1) or PIM1 overexpressing vector (MigPIM1). **B**, Relative RNA expression of KLF4, NANOG, SOX2 and OCT-4 in PC3 and DU145 cells transduced with empty vector (EV) or PIM1 vector (PIM1). **C**, WB using the identified antibodies on murine prostate epithelial tumor cells (mPrEC) cells in which Trp53 and Rb1 had been knocked out, and stably transduced with empty vector plasmid (EV) or FUCRW-PIM1 (PIM1) plasmid. **D**, Relative OCT-4 RNA expression in Dox-inducible PC3-Tripz-PIM1 after Dox treatment (20ng/ml, 48h). Relative Firefly/Renilla luciferase activity measurement after Dox treatment (20ng/ml, 48h) in PC3-Tripz-PIM1 cells transfected with luciferase reporter plasmid (p-OCT-4-Luc) controlled by OCT-4 proximal (Proximal) and distal (Distal) enhancers. Untransfected PC3-Tripz-PIM1 cells were used as control. **A,B,D,** Relative RNA expression were normalized to 18S RNA levels. Values are mean +/- SEM; n=3; n.s.= not significant, *p<0.05, **p<0.01.

Figure 4. PIM1 controls H19 expression and regulates tumor growth. A, Mouse prostate organoid cells transduced with empty vector (EV-RFP) or FUCRW-PIM1 plasmid (PIM1-RFP) (5000/well) were plated for organoid growth analysis. Representative images of the growth analysis (left panel), scale bar: 1000µm. Quantification of the organoid growth (right panel). **B**, Relative RNA levels of Pim1, H19, Klf4, Oct-4, Sox2 in mouse prostate organoids described in A. Relative RNA expression was normalized to Hprt RNA. **C**, Relative RNA expression of NANOG, OCT-4, SOX2, and KLF4 in PC3-LN4 cells transfected with a control siRNA (si-C) and siRNA to knockdown H19 (si-H19). Relative RNA expression levels were normalized to ACTIN RNA. **D**, Relative RNA expression of H19, KLF4, NANOG, OCT-4 and SOX2 in SUP-T1E cells transfected with control MigR1 vector (MigR1) or PIM1 overexpressing vector (MigPIM1). Mig PIM1 cells were further transduced with shSCr and shH19. **E,** Relative H19 RNA expression in HSB-2, DU.528 and CUTLL1 after PIM-i treatment (AZD1208, 3µM, 24h). DMSO was used for control treatment. Relative RNA expression levels were normalized to ACTIN RNA. WB of these cells with indicated antibodies for validation of PIM1 inhibition. **F**, Relative H19 RNA expression in LNCaP cells treated with PIM-i (PIM447, 1 µM, 24h). DMSO was used for control treatment. Relative RNA expression was normalized to 18S RNA unless specified otherwise. Values are mean +/- SEM; n=3; n.s.= not significant, *p<0.05, **p<0.01, ***p<0.001.

Figure 5. PIM inhibitor represses growth in combination with inhibition of H19 and sensitizes LNCaP cells to enzalutamide. A, Cell viability measured by XTT assay of PC3 cells treated with si-H19 and PIM-i (PIM-447, 0.5μM, 72h). DMSO was used for the control treatment. Cell viability is represented as normalized growth (DMSO=1). **B**, Bar graphs showing growth response measured as percent average organoid area, of OWCM-155 NEPC organoids with and without knockdown of H19 (Lv-shH19 vs Lv-scr) in combination with PIM1-i (PIM447, 3μM, 4 days). DMSO was used for control treatment. **C**, Percent cell viability of LNCaP cells stably expressing empty vector (EV) or FUCRW-PIM1 plasmid (PIM1), treated with Enza (MDV3100, 10μM, 48h). DMSO treatment was used as control. **D**, Cell viability of LNCaP cells stably expressing empty vector (LNCaP-EV) treated with increasing concentrations of either Enza (MDV3100, 2μM and 5μM) or PIM-i (PIM447, 0.3μM and 1μM, 72h) and combination, measured by XTT assay. DMSO was used to treat cells when no drug was added (0μM). Values are mean +/- SEM; n=3; σ represents p values<0.05 as compared to DMSO treatment. # represents p values<0.05 as compared to 2μM Enza. Ψ represents p values<0.05 as compared to 5μM Enza. *p<0.05, **p<0.01, **E**, Cell viability of LNCaP cells stably overexpressing H19 (LNCaP-H19) treated with Enza or PIM-i and combination, as stated in D. XTT assay was carried out 72h after the start of drug treatment and absorbance was measured at 450nm. Results from cell viability in D and E were represented as absorbance at 450nm. Values are mean +/- SEM; n=3; n.s.= not significant, *p<0.05, **p<0.01, ***p<0.001.

Figure 1

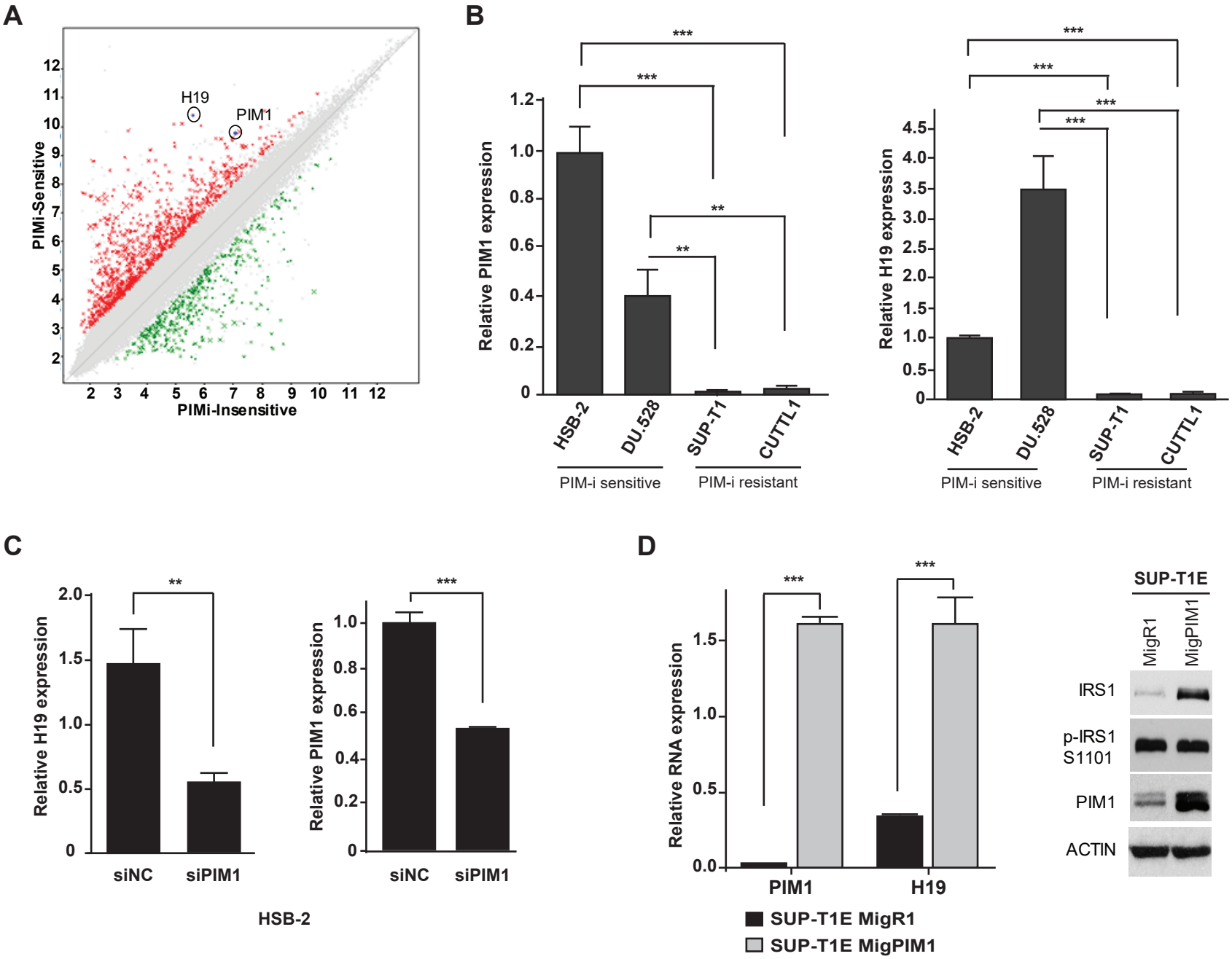
A
H19
PIM1
PIMi-Sensitive
PIMi-Insensitive
B
Relative PIM1 expression
HSB-2
DU.528
SUP-T1
CUTTL1
PIM-i sensitive
PIM-i resistant
Relative H19 expression
C
Relative H19 expression
siNC
siPIM1
HSB-2
Relative PIM1 expression
D
Relative RNA expression
PIM1
H19
SUP-T1E MigR1
SUP-T1E MigPIM1
SUP-T1E
MigR1
MigPIM1
IRS1
p-IRS1 S1101
PIM1
ACTIN

Figure 2

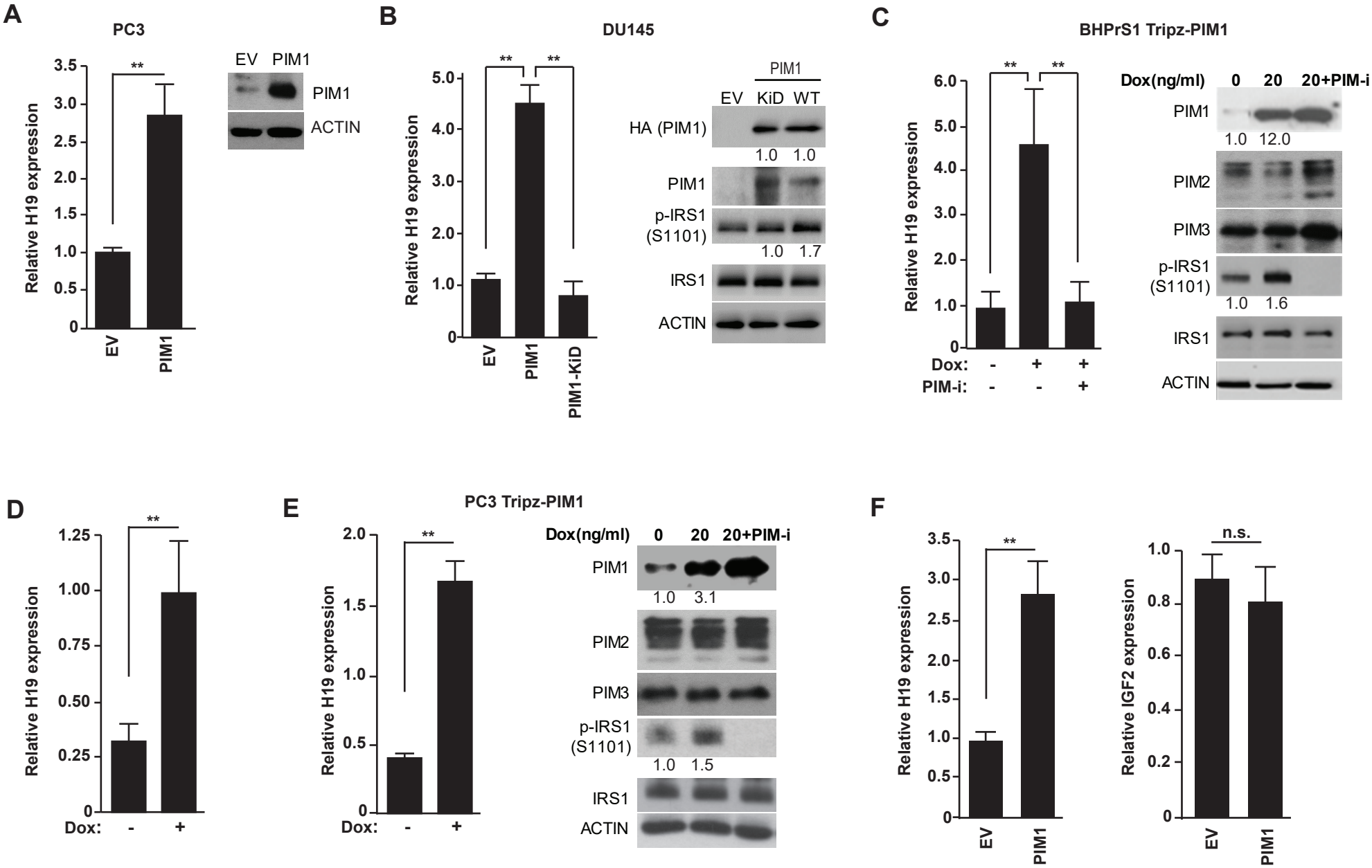
A
PC3
Relative H19 expression
EV
PIM1
**
EV PIM1
PIM1
ACTIN
B
DU145
Relative H19 expression
EV
PIM1
PIM1-KiD
**
**
PIM1
EV KiD WT
HA (PIM1)
1.0 1.0
PIM1
p-IRS1 (S1101)
1.0 1.7
IRS1
ACTIN
C
BHPrS1 Tripz-PIM1
Relative H19 expression
Dox: - + +
PIM-i: - - +
**
**
Dox(ng/ml) 0 20 20+PIM-i
PIM1
1.0 12.0
PIM2
PIM3
p-IRS1 (S1101)
1.0 1.6
IRS1
ACTIN
D
Relative H19 expression
Dox: - +
**
E
PC3 Tripz-PIM1
Relative H19 expression
Dox: - +
**
Dox(ng/ml) 0 20 20+PIM-i
PIM1
1.0 3.1
PIM2
PIM3
p-IRS1 (S1101)
1.0 1.5
IRS1
ACTIN
F
Relative H19 expression
EV
PIM1
**
Relative IGF2 expression
EV
PIM1
n.s.

Figure 3

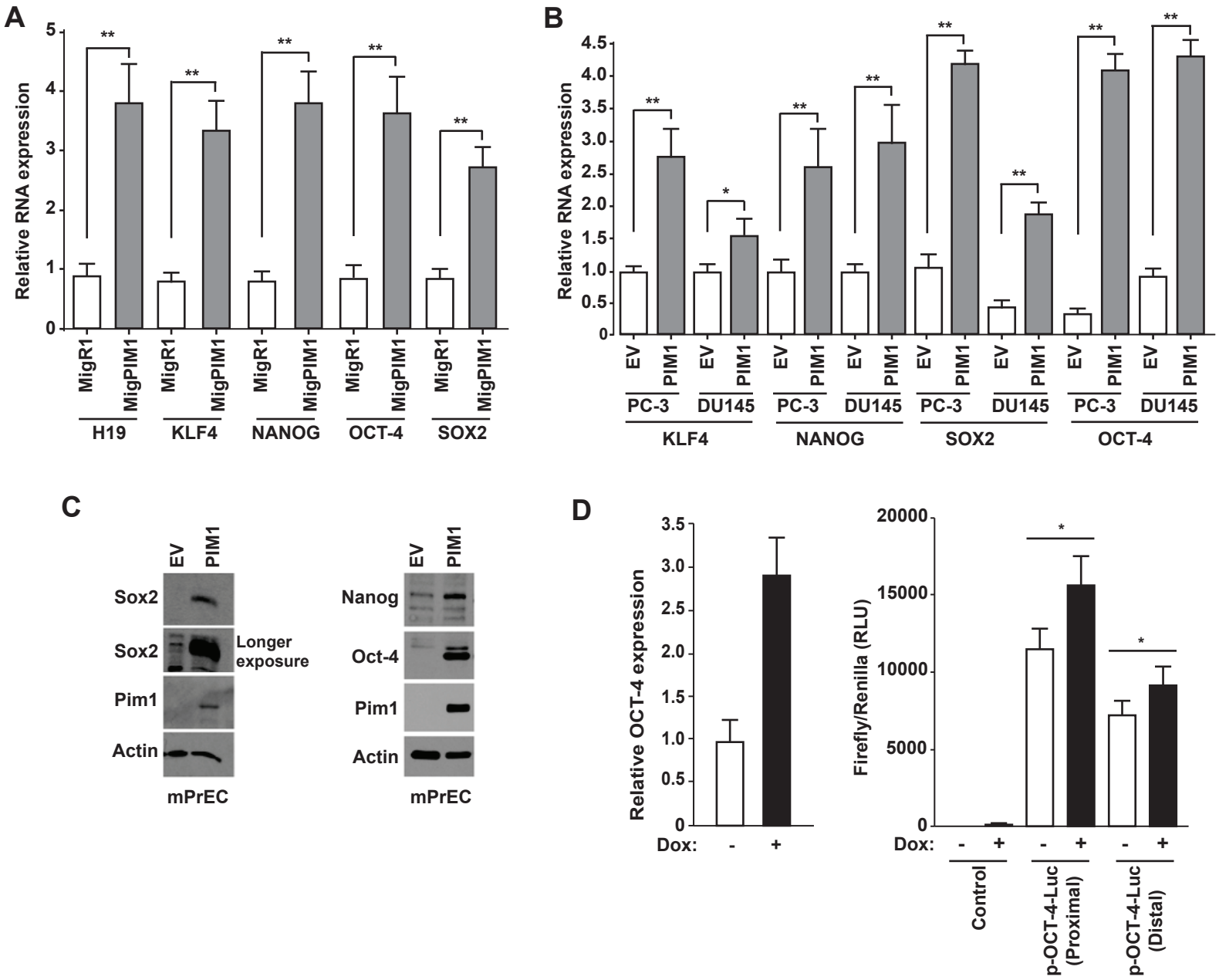
A
Relative RNA expression
MigR1
MigPIM1
H19
KLF4
NANOG
OCT-4
SOX2
B
Relative RNA expression
EV
PIM1
PC-3
DU145
KLF4
NANOG
SOX2
OCT-4
C
EV
PIM1
Sox2
Sox2
Longer exposure
Pim1
Actin
mPrEC
Nanog
Oct-4
Pim1
Actin
mPrEC
D
Relative OCT-4 expression
Dox:
Firefly/Renilla (RLU)
Control
p-OCT-4-Luc (Proximal)
p-OCT-4-Luc (Distal)

Figure 4

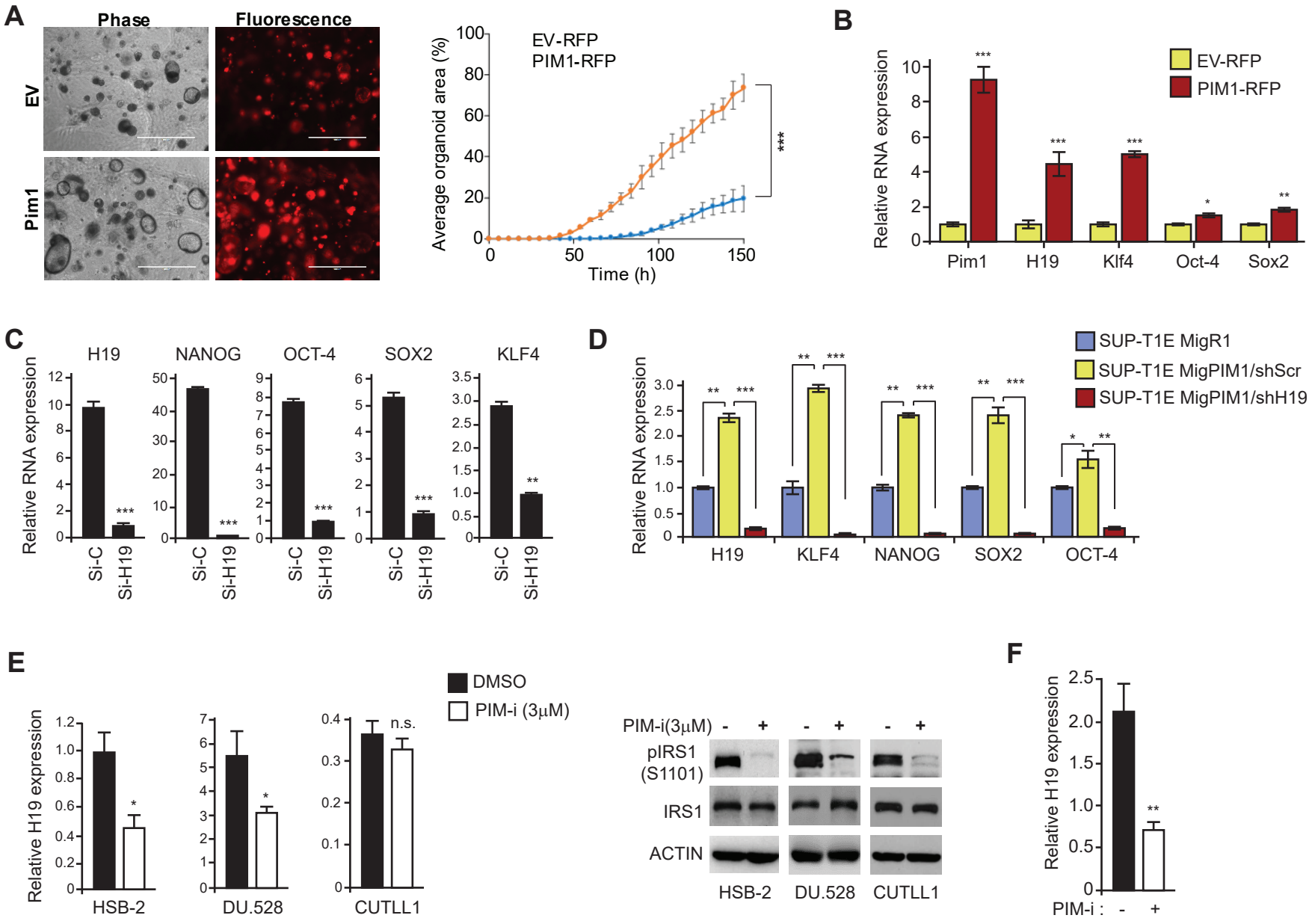
A
Phase
Fluorescence
EV
Pim1
EV-RFP
PIM1-RFP
Average organoid area (%)
Time (h)
B
Relative RNA expression
EV-RFP
PIM1-RFP
Pim1
H19
Klf4
Oct-4
Sox2
C
H19
NANOG
OCT-4
SOX2
KLF4
Relative RNA expression
Si-C
Si-H19
D
SUP-T1E MigR1
SUP-T1E MigPIM1/shScr
SUP-T1E MigPIM1/shH19
Relative RNA expression
H19
KLF4
NANOG
SOX2
OCT-4
E
DMSO
PIM-i (3μM)
Relative H19 expression
HSB-2
DU.528
CUTLL1
n.s.
PIM-i(3μM)
pIRS1 (S1101)
IRS1
ACTIN
F
Relative H19 expression
PIM-i :

Figure 5

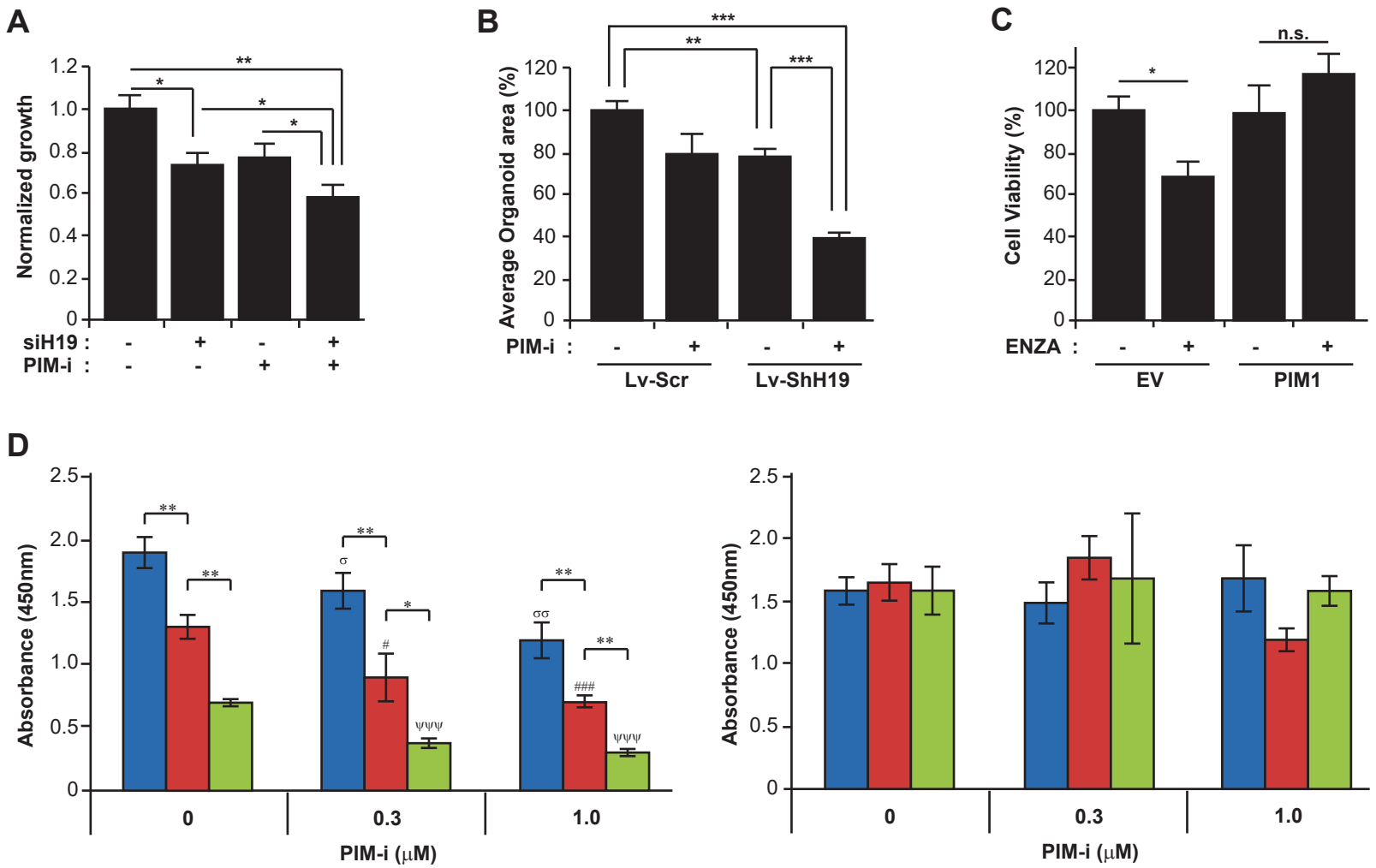
A
Normalized growth
siH19 :
PIM-i :
B
Average Organoid area (%)
PIM-i :
Lv-Scr
Lv-ShH19
C
Cell Viability (%)
n.s.
ENZA :
EV
PIM1
D
Absorbance (450nm)
PIM-i (μM)
Absorbance (450nm)
PIM-i (μM)

PIM protein kinases regulate the level of the long noncoding RNA H19 to control stem cell gene transcription and modulate tumor growth

Neha Singh[1], Sathish K.R. Padi[1] , Jeremiah J. Bearss[1], Ritu Pandey[1,2], Himisha Beltran [4] , Koichi Okumura, Jin H. Song[1,2], Andrew S. Kraft[1,3*] and Virginie Olive[1*,]

[1]University of Arizona Cancer Center, University of Arizona, 1515 N. Campbell Ave. Tucson, AZ, USA 85724

[2]Department of Cellular and Molecular Medicine, University of Arizona, 1515 N Campbell Avenue, Tucson, AZ, USA 85724

[3]Department of Medicine, University of Arizona, 1515 N Campbell Avenue, Tucson, AZ, USA 85724

[4]Department of Medical Oncology, Dana-Farber Cancer Institute, 44 Binney St, Boston MA 02115

***Corresponding authors**

Supporting information Appendix:

Supplementary Figures S1- S9

Supplementary table S1: Due to large size the Table S1 has not been included in this attachment and is available upon request.

Supplementary table S2

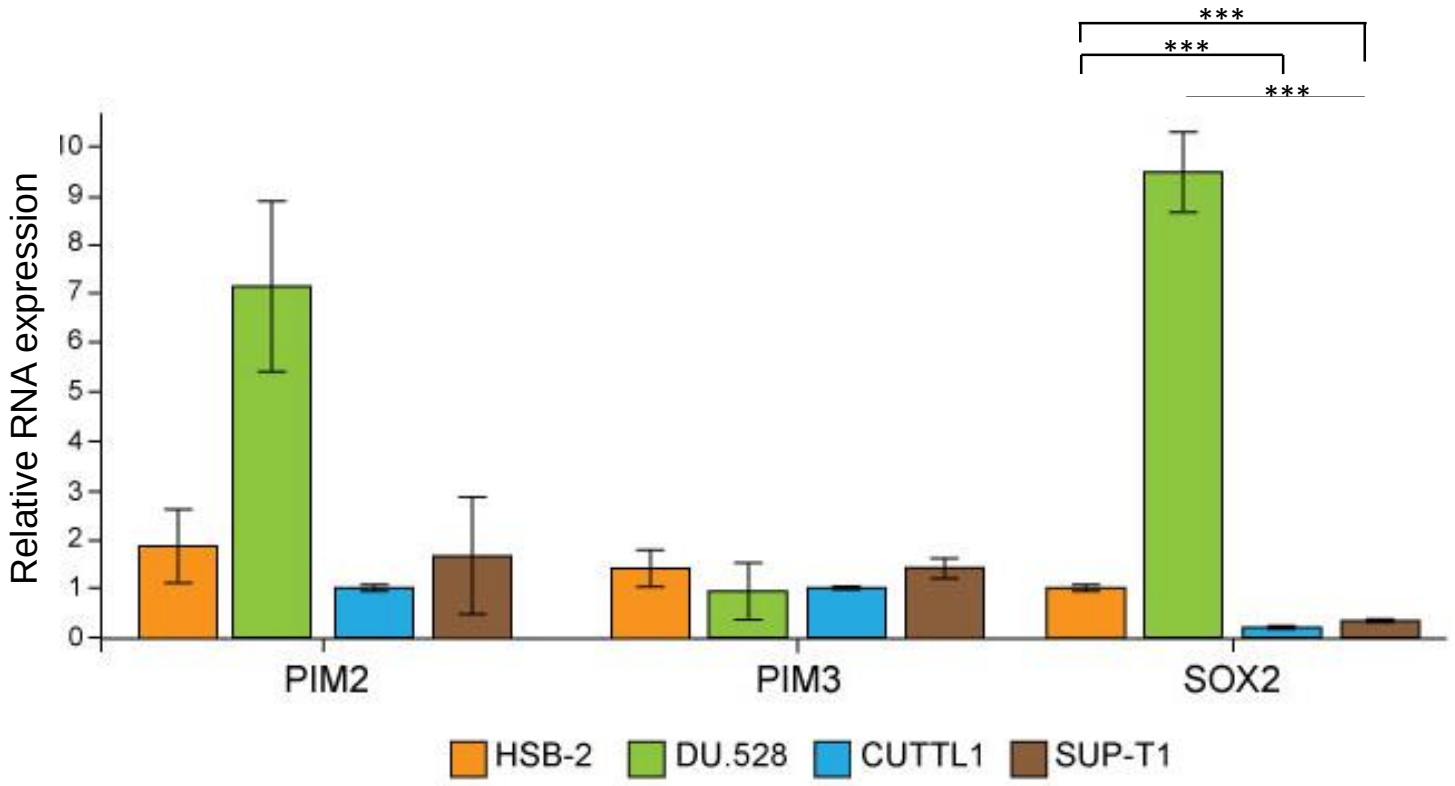

Figure S1: Increased expression of PIM2 in PIM-i sensitive vs resistant T-ALL. Relative mRNA expression of PIM2, PIM3 and SOX2 in indicated T-ALL cell lines. RNA expression are normalized to 18S RNA. Data are mean +/- S.D., n=3, ***p<0.001.

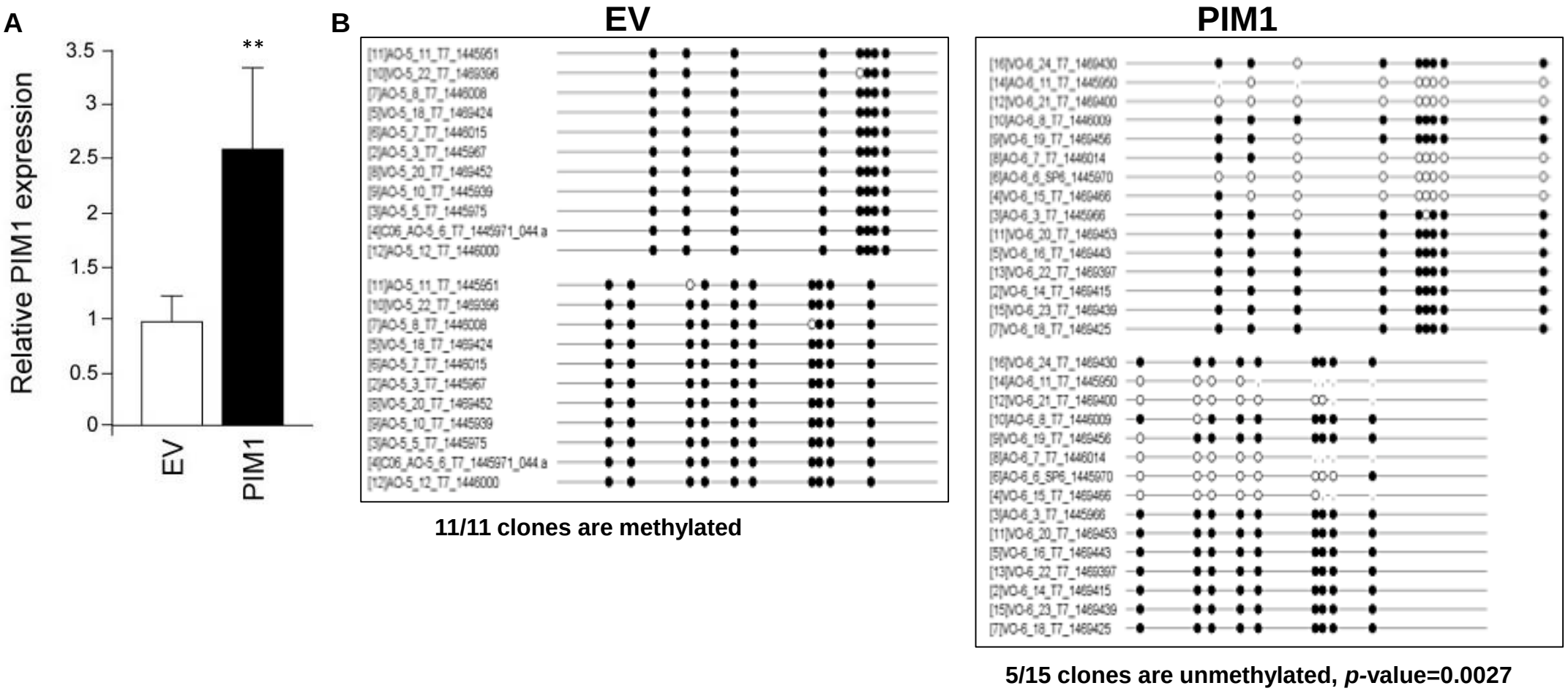

Figure S2: PIM1 decreased the DNA methylation of H19 DMR in SUPT1 cells. A. Relative H19 RNA expression after PIM1 overexpression in SUP-T1E cells versus control vector expressing cells. RNA levels were normalized to 18S RNA. Data are mean +/- S.D., n=3, **p<0.01. **B.** Bisulfite sequencing of H19 DMR in SUP-T1E cells overexpressing PIM1 or an empty vector (as control). Eleven SUP-T1E control clones and fifteen overexpressing PIM1 clones were sequenced. Dark circles represent methylated CpG and open circles unmethylated CpG.

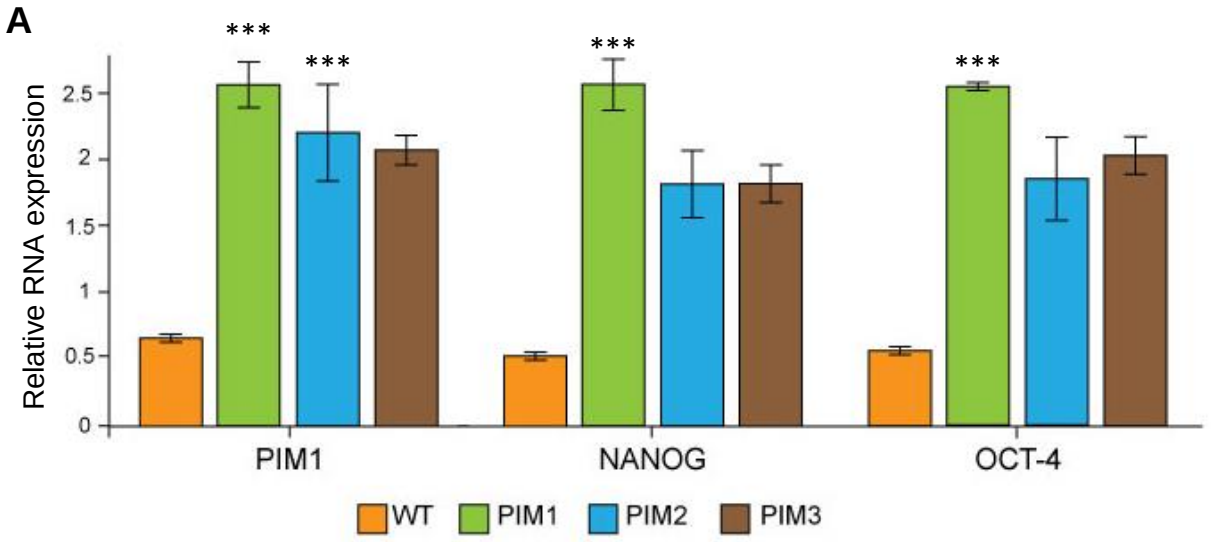

Figure S3: PIM1 overexpression induces a stem cell like phenotype in PC3 cells. A, Relative RNA levels of H19, NANOG and OCT-4 in PC3 cells transiently transfected with FUCRW vectors expressing either PIM1, PIM2 or PIM3. WT cells were used as control. Relative RNA expression are normalized to 18S RNA. Data are mean +/- S.D., n=3, **p<0.01, ***p<0.001 w.r.t. controls (WT). **B**, Expression of the indicated stem cell markers upon PIM1 overexpression in PC3 cells followed 48h later by measurement of CD29, CD49b and CD24 surface markers by FACS. Data are mean +/- S.D., n=3.

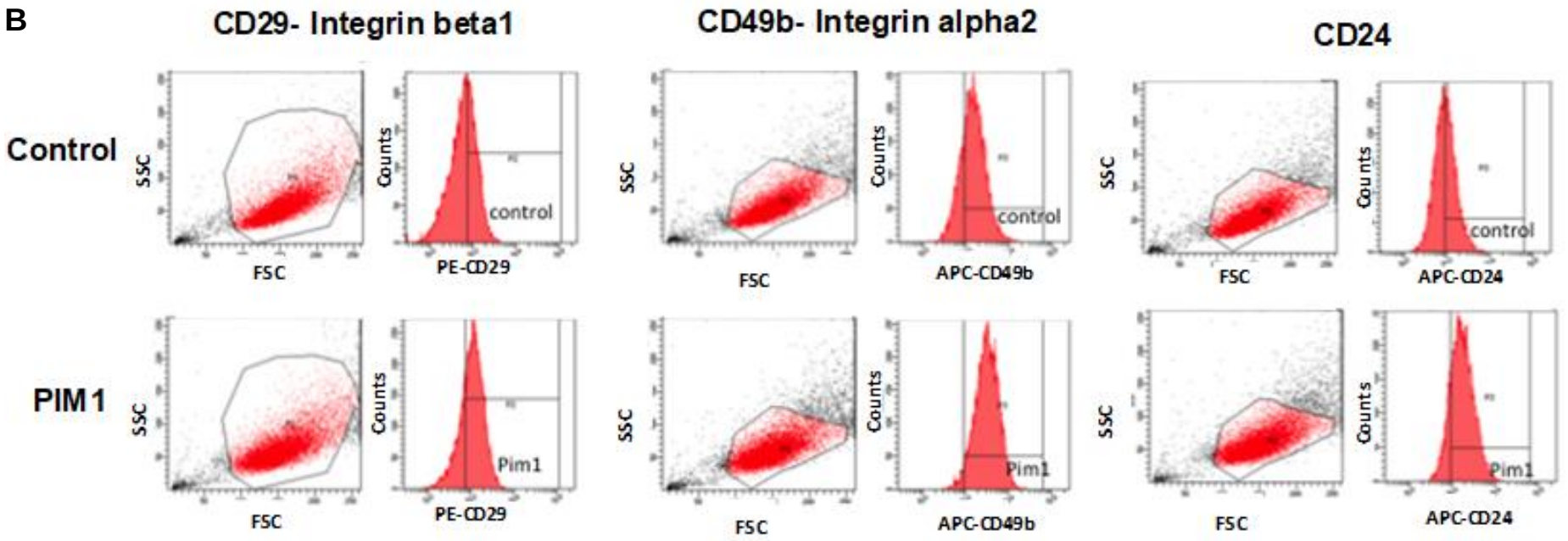

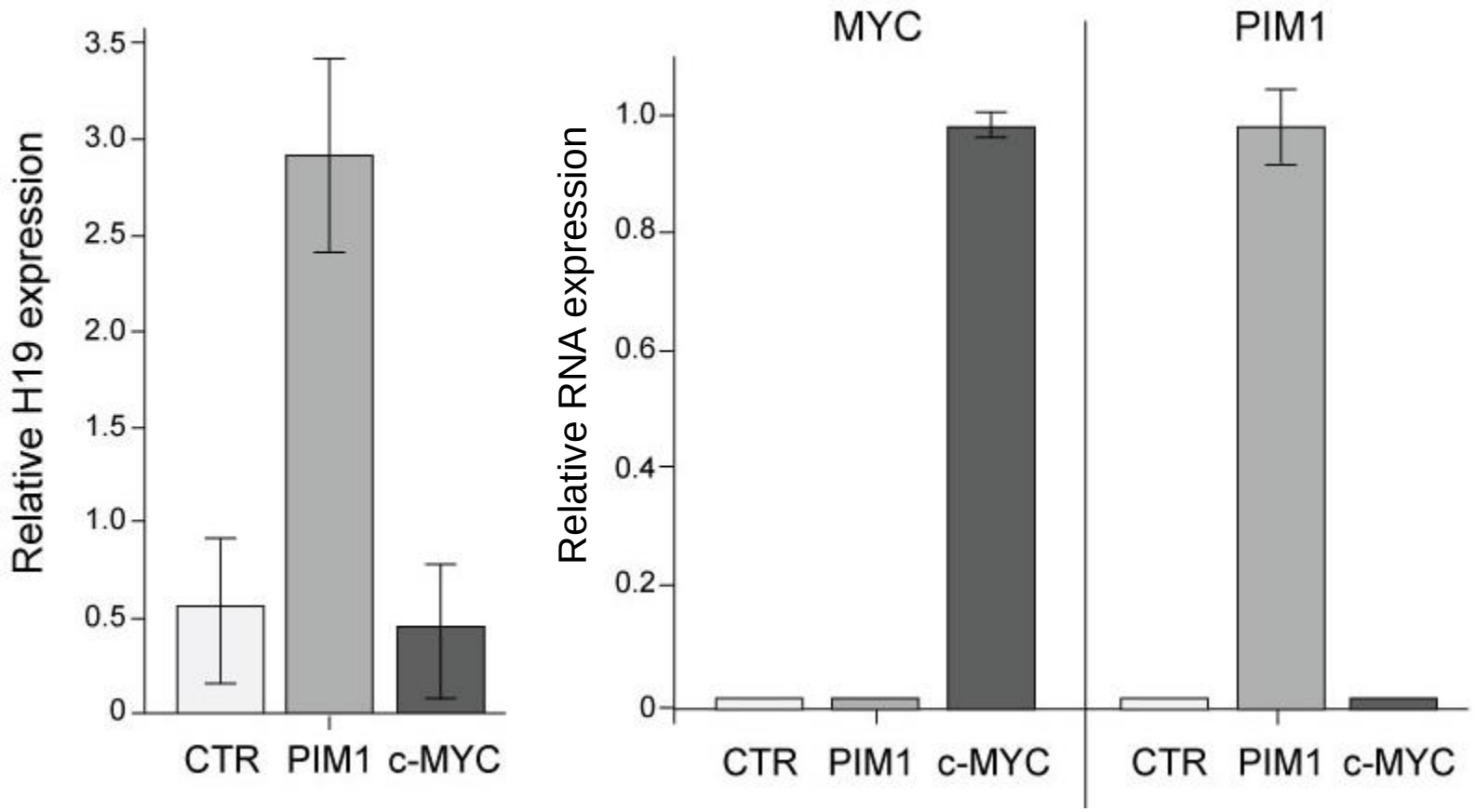

Figure S4: c-MYC expression has no effect on H19 levels. PIM1 or c-MYC were transiently overexpressed in DU145 cells. H19 levels are shown after PIM1 or c-MYC transfection. RNA level are normalized to 18S RNA (left panel). PIM1 and c-MYC RNA levels measured after transfection (right panel). Data are mean +/- S.D., n=3, **p<0.01, ***p<0.001 control (CTR).

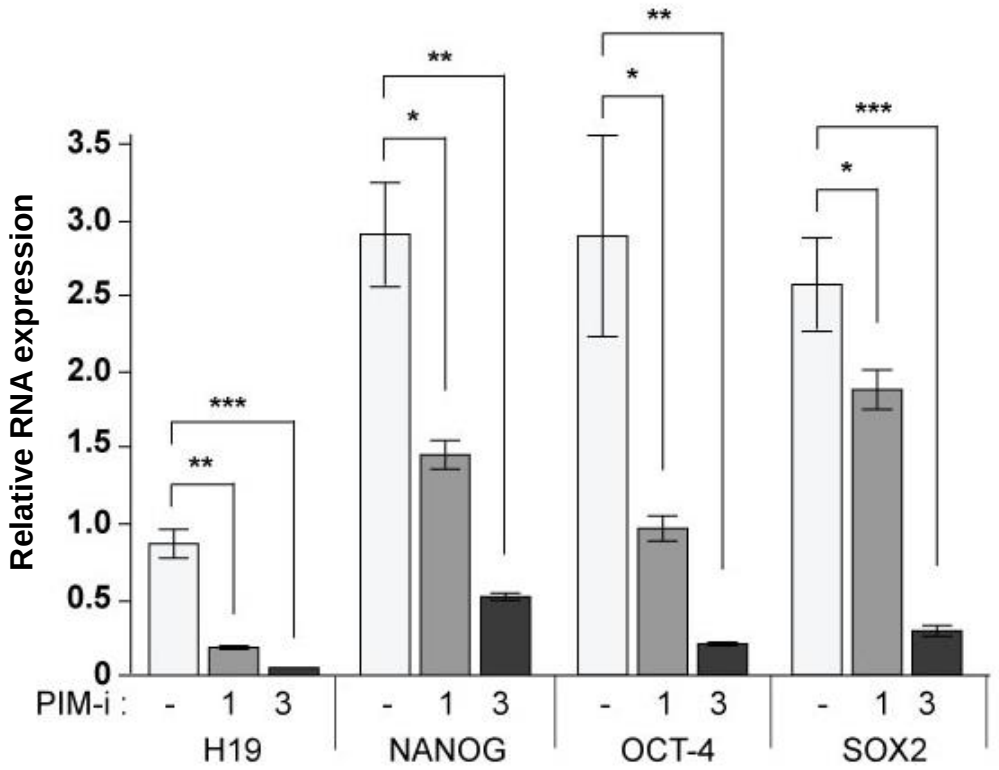

Figure S5: Pharmacological inhibition of PIM kinases reduces stem cell gene expression in NEPC cell line. Relative mRNA expression of H19, NANOG, OCT-4 and SOX2 in neuroendocrine prostate cancer (NEPC) cell line LASCPC-01 treated with DMSO or PIM-i (PIM447, 1μM and 3μM). RNA expression are normalized to 18S RNA. Data are mean +/- S.D., n=3, *p<0.05, **p<0.01, ***p<0.001**.**

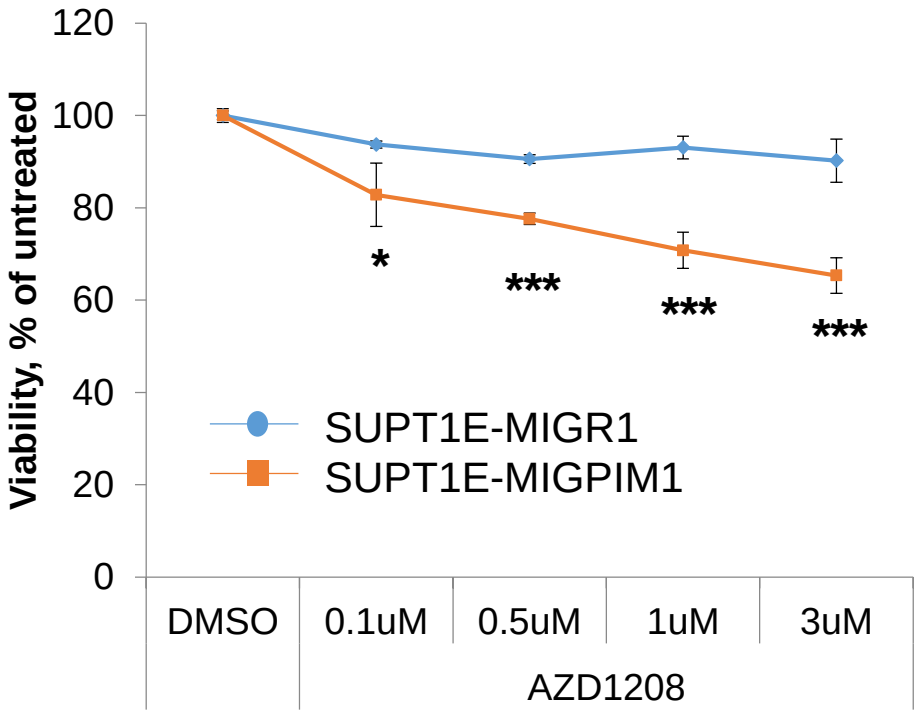

Figure S6: PIM1 overexpression restores partial sensitivity in PIM-i resistant T-ALL cells. Percent viability of SUPT1E cells after MIGR1 and MIGPIM1 transduction, treated with PIM-i (AZD1208) at the indicated doses. DMSO was used as control. Data are mean +/- S.D., n=3, *p<0.05, **p<0.01, ***p<0.001 vs. SUP-T1E-MIGR1.

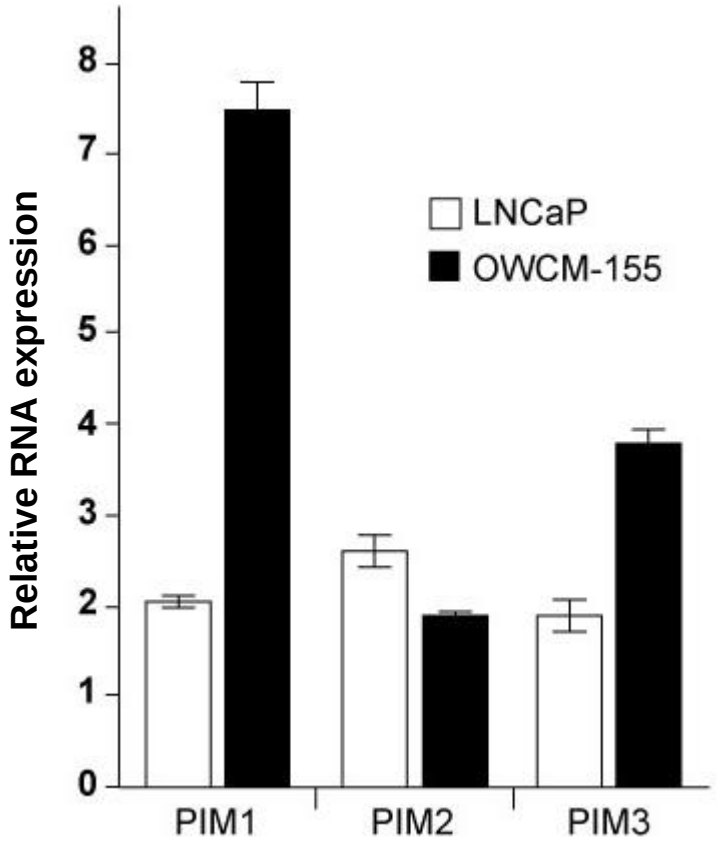

Figure S7: PIM kinase is highly expressed in NEPC. Relative RNA expression of PIM1/2/3 in OWCM-155 NEPC organoids and androgen responsive adenocarcinoma cell line LNCaP. RNA expression are normalized to 18S RNA. Data are mean +/- S.D., n=3.

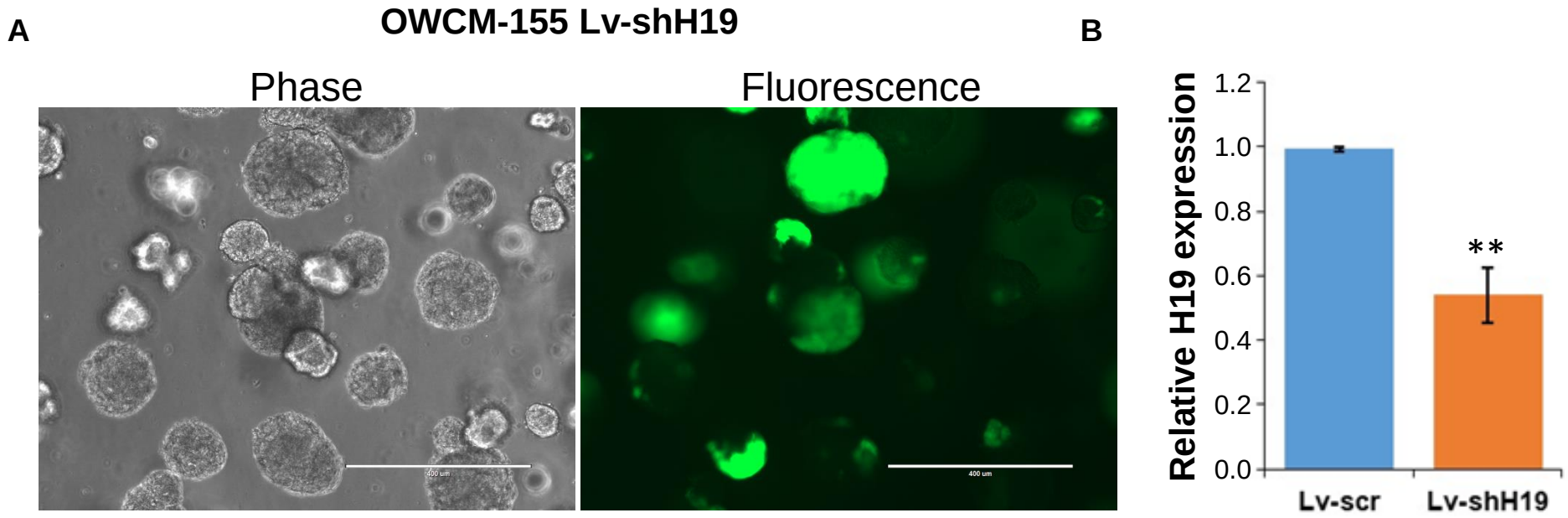

Figure S8: Knockdown of H19 expression in NEPC organoid OWCM-155. A, Representative images of lentiviral transduction of OWCM-155 with GFP expressing lentiviral plasmid pLenti-siH19-GFP, scale bar: 400µm. **B.** Relative H19 RNA expression in OWCM-155 transduced with control (Lv-scr) or H19 KD (Lv-shH19) lentivector. Relative H19 expression was normalized to 18S RNA. Values are mean +/- S.D. ** represents p-value <0.01.

A

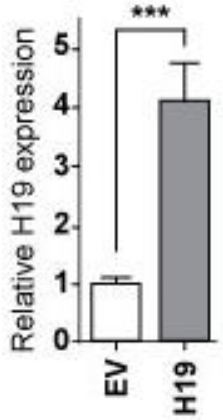

B

Dose ENZA	Dose PIM-i	Effect	Combination Index
2.0 μM	0.3 μM	0.52962	0.66509
2.0 μM	1.0 μM	0.63415	0.66455
5.0 μM	0.3 μM	0.80662	0.35645
5.0 μM	1.0 μM	0.84321	0.34847

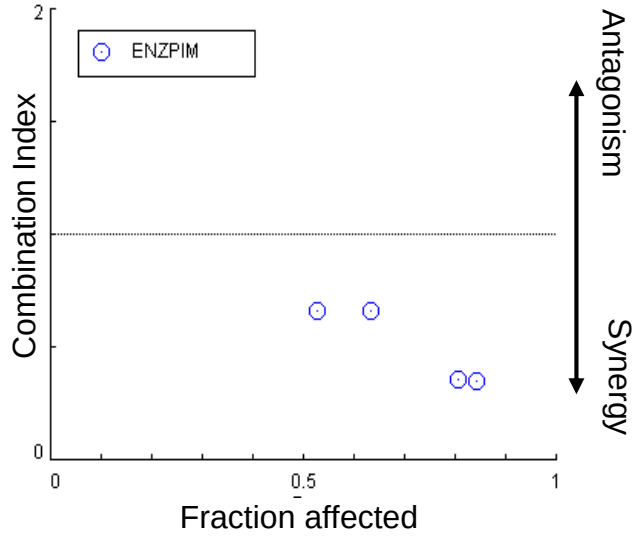

Figure S9: Synergistic effect of pan-PIM inhibitor(s) with Enzalutamide in LNCaP/H19. A, Relative H19 levels in LNCaP cells transduced with EV and H19. RNA expression is normalized to 18S RNA. Data are mean +/- S.D., n=3, ***p<0.001. **B**, LNCaP and LNCaP/H19 cells were treated with PIM447 either alone or in combination with Enza for 72 h and percentage viable cells was determined by XTT assay. The percent growth inhibition of drugs alone and in combination was determined and the combination index (CI) for Enza 2μM/ 5μM at the indicated concentrations of PIM447 was determined by Combosyn plot. The combination index value of below 1 indicates synergism.

Table S2: Pathway analysis of transcriptomes from Microarray data from 6 T-ALL cell lines: Results indicate the pathways enriched for significantly up or downregulated genes when comparing PIM-i sensitive vs resistant T-ALL cell lines.

Pathway	#Total	#Up-regulated	List of upregulated genes	#Down-regulated	List of downregulated genes	p-value
Chemokine signaling pathway	17	16	CCL22,PRKCB,JAK2,PREX1,NFKB1,CCR1,JAK3,CCL1,PIK3CD,CCR7,PIK3R5,CCR4,ADCY7,XCL1,TIAM2,ARRB1	1	PIK3CG	0.00019
VEGFA-VEGFR2 Signaling	33	29	MAPK8,FAS,BIN1,SMARCA2,GAB1,PRKCB,FOXO1,PTPRJ,TXNIP,CTNNA1,MAP3K5,NFATC2,EGR1,BMP10,NFKB1,ICAM1,ADAMTS1,ACKR3,FGD5,LMO2,IER5,ZNF555,CCRL2,TRPC3,CYBB,SET,SHROOM2,FSCN1,NEXN	4	MLLT4,PRKAA2,ANXA1,OCLN	0.0002
IL-4 Signaling Pathway	7	6	JAK2,NFKB1,SOCS1,IL4R,PIK3CD,JAK3	1	IL4	0.00548
Interleukin-11 Signaling Pathway	6	6	JAK2,PPP2R4,RPS6KA1,RUNX2,ICAM1,ITGA2	0		0.00592
JAK/STAT	10	7	CISH,RPS6KA1,JAK2,NFKB1,FOXO1,SOCS2,MAPK8	3	PDE3B,PIK3CG,PRKAA2	0.0073
TGF-beta Signaling Pathway	10	8	MAPK8,CDKN1A,PJA1,PRKAR2A,CAV1,ITGA2,TGFBR3,RUNX2	2	DAB2,SPTBN1	0.03774
ESC Pluripotency Pathways	9	7	SMAD5,ACVR1,BMPR2,PIK3CD,LIF,GAB1,SMAD6	2	SMAD1,FZD3	0.04317
PI3K-Akt Signaling Pathway	20	16	CCND2,JAK3,JAK2,COL6A3,ITGA2,IL4R,PIK3CD,PIK3R5,ANGPT1,VEGFC,F2R,LPAR6,CDKN1A,CREB3L1,NFKB1,BCL2L11	4	PIK3CG,PRKAA2,PHLPP1,IL4	0.04505

Insulin Signaling	11	8	PIK3CD,MAP3K5,MAP3K8,RPS6KA1,MAPK8,SOCS1,GAB1,EGR1	3	PIK3CG,PRKAA2,KIF3A	0.05809
MAPK Signaling Pathway	15	14	TNF,ARRB1,MAP3K8,MAPK8,RRAS,RRAS2,NFKB1,RASGRP3,STK3,FAS,MAP3K5,DUSP6,MAPKAPK3,CACNA1D	1	DUSP10	0.06204
Hematopoietic Stem Cell Differentiation	7	7	NFATC2,LMO2,PIM1,HLF,ZFP37,TXK,F2R	0		0.08813